Patterns of flavor signals in supersymmetric models

Toru Goto,[1,2,*] Yasuhiro Okada,[1,3,†] Tetsuo Shindou,[4,5,‡] and Minoru Tanaka[6,§]

[1]*Theory Group, KEK, Tsukuba, Ibaraki 305-0801, Japan*[‖]

[2]*YITP, Kyoto University, Kyoto 606-8502, Japan*

[3]*Department of Particle and Nuclear Physics, The Graduate University for Advanced Studies (Sokendai), Tsukuba, Ibaraki 305-0801, Japan*

[4]*DESY Theory Group, Notkestrasse 85, D22607 Hamburg, Germany*[‖]

[5]*SISSA/ISAS, via Beirut 2-4, I-34014 Trieste, Italy*

[6]*Department of Physics, Graduate School of Science, Osaka University, Toyonaka, Osaka 560-0043, Japan*

(Received 19 November 2007; published 14 May 2008)

Quark and lepton flavor signals are studied in four supersymmetric models, namely, the minimal supergravity model, the minimal supersymmetric standard model with right-handed neutrinos, SU(5) supersymmetric grand unified theory with right-handed neutrinos, and the minimal supersymmetric standard model with U(2) flavor symmetry. We calculate $b \to s(d)$ transition observables in B_d and B_s decays, taking the constraint from the $B_s - \bar{B}_s$ mixing recently observed at the Tevatron into account. We also calculate lepton flavor violating processes $\mu \to e\gamma$, $\tau \to \mu\gamma$, and $\tau \to e\gamma$ for the models with right-handed neutrinos. We investigate possibilities to distinguish the flavor structure of the supersymmetry breaking sector with use of patterns of various flavor signals which are expected to be measured in experiments such as MEG, LHCb, and a future Super B factory.

DOI: 10.1103/PhysRevD.77.095010 PACS numbers: 12.60.Jv, 11.30.Er, 12.15.Hh, 14.40.Nd

I. INTRODUCTION

The problem of flavors is one of the interesting aspects of particle physics. Results obtained at B factory experiments so far indicate that the Cabibbo-Kobayashi-Maskawa (CKM) mixing [1] is the main mechanism of flavor mixing phenomena in the quark sector, although there still remains some room for new physics beyond the standard model (SM). On the other hand, in the lepton sector, neutrino experiments unveil large flavor mixings quite different from the quark sector [2–5]. These mixings in the lepton sector are certainly beyond the SM, suggesting a new mechanism of flavor mixing. It is clear that flavor physics is a clue to new physics.

In the coming years, we expect new experimental results from the energy frontier, that is, the CERN Large Hadron Collider (LHC) [6]. LHC experiments will provide us with invaluable information on new physics. Among several candidates of new physics, supersymmetry (SUSY) is the most attractive and widely discussed [7]. It is possible that some of the superparticles are discovered in the early stage of LHC experiments.

One of the key questions in realistic SUSY models is to identify the mechanism of SUSY breaking. The SUSY breaking mechanism can be explored by determining the SUSY mass spectrum in LHC experiments at the energy frontier. On the other hand, the whole flavor structure of the SUSY breaking cannot be determined by the energy frontier experiment alone. There is no *a priori* reason to exclude flavor changing soft SUSY breaking terms in the squark and the slepton sectors, and some of them are already strongly restricted by the existing low-energy experimental data [8,9]. It means that we can extract important aspects of the SUSY breaking mechanism from flavor physics.

Two new flavor experiments are under construction, and several others are proposed. The MEG experiment [10], which intends to search for the lepton flavor violating (LFV) process $\mu \to e\gamma$ at a branching ratio down to 10^{-13}, will start data taking soon. The LHCb experiment [11,12] is another dedicated flavor experiment under construction and will be ready by the LHC startup in 2008. It is designed to observe several rare decays and CP violations in B and B_s decays. There are plans of future Super B factories under discussion [13–15]. In addition to measure several B decay observables with higher statistics, it is expected to search for LFV processes in tau decays at a branching ratio of 10^{-9}. These new flavor experiments themselves and their interplay with LHC experiments at the energy frontier will augment our knowledge on flavors and eventually new physics.

Several strategies are possible in order to study the implication of the past and present experimental data on SUSY models and predictions of flavor signals in future experiments. One of them is a model-independent method based on the mass insertion [16–18]. In this approach, a general set of off-diagonal matrix elements (mass insertions) of the squarks and the sleptons is assumed, and one (or two) of the elements is (are) activated in order to obtain a bound from a specific experiment. Repeating this procedure for every relevant experiment, a list of bounds for the

*tgoto@post.kek.jp
†yasuhiro.okada@kek.jp
‡tetsuo.shindou@desy.de
§tanaka@phys.sci.osaka-u.ac.jp
‖Present address.

possible mass insertions is obtained. This list is used to evaluate flavor signals in future experiments. As an opposite way, a model-specific analysis is possible [19–26]. In this approach, one specifies a SUSY model with a well-defined SUSY breaking sector and analyzes one (or more) selected flavor signal(s). In this way one can make definite predictions on observable quantities in flavor changing processes provided that the relevant model parameters are given.

In our previous works [27,28], we adopted a different approach. We selected three well-motivated SUSY models: the minimal supergravity (mSUGRA), the SU(5) SUSY grand unified theory (GUT) with right-handed neutrinos, and the minimal supersymmetric standard model (MSSM) with U(2) flavor symmetry. Each of these models has a distinct flavor structure in its SUSY breaking sector at the electroweak scale. Then, we investigated various flavor signals in these models in a unified fashion. This approach allows us to evaluate flavor signals definitely and to discuss the possibility to distinguish several different flavor structures in the SUSY breaking sector in future flavor experiments. The quark flavor signals which we studied are the CP violation parameter ε_K in the $K^0 - \bar{K}^0$ mixing, the $B_d - \bar{B}_d$ and the $B_s - \bar{B}_s$ mass splittings (Δm_{B_d} and Δm_{B_s} respectively), CP asymmetries in $B \to J/\psi K_S$ and related modes, the direct and the mixing-induced CP asymmetries in $b \to s\gamma$, and the CP asymmetry in $B \to \phi K_S$. In addition, an LFV process $\mu \to e\gamma$ was studied. Comparing predictions of the models with each other, we showed that the study of quark flavor signals at low energies could discriminate several SUSY models that have different flavor structures in their SUSY breaking sectors.

In the present work, we extend our previous works. New features and improvements of the present work are the following:

(i) In addition to the three models, we consider the MSSM with right-handed neutrinos and the seesaw mechanism without GUT.
(ii) Three cases of the low-energy neutrino mass spectrum and three types of Ansätze for the neutrino Yukawa coupling matrix are studied.
(iii) New and up-to-date experimental data are incorporated. In particular Δm_{B_s} measured by the CDF and D0 experiments at Fermilab Tevatron affects predictions of several B decay modes [18,29].
(iv) LFV tau decays and their implications are examined.
(v) As computational improvements, two-loop renormalization group equations for the MSSM (with right-handed neutrinos) parameter running and one-loop threshold corrections at the electroweak scale are implemented.

With these new features and improvements, we pursue the possibility to distinguish the flavor structure of the SUSY breaking sector by low-energy flavor experiments and to understand the SUSY breaking mechanism consequently.

A brief summary of our analysis is as follows. We expect significant flavor signals in the lepton sector for the models with right-handed neutrinos if the neutrino Yukawa coupling is $O(1)$. In the MSSM with right-handed neutrinos, depending on the texture of the neutrino Yukawa coupling matrix, some of the LFV processes, $\mu \to e\gamma$, $\tau \to \mu\gamma$, and $\tau \to e\gamma$, could be discovered in the near future. In the SU(5) SUSY GUT with right-handed neutrinos, in addition to the above texture dependent signals, $\mu \to e\gamma$ can be close to the present experimental bound due to GUT interactions. As for the quark flavor signals, CP violating asymmetries in $b \to s$ and $b \to d$ transitions can be significant in the SU(5) SUSY GUT with right-handed neutrinos and in the U(2) model. Enhanced modes vary according to the texture of the neutrino Yukawa coupling matrix in the SU(5) SUSY GUT with right-handed neutrinos. Our analysis indicates that clarifying a pattern of the quark and lepton flavor signals is an important step to determine the correct SUSY model.

This paper is organized as follows. In Sec. II, the models are presented and the relevant SUSY parameters are introduced. Our numerical analysis with the experimental inputs and the outline of computational procedure are shown in Sec. III. Conclusions are given in Sec. IV.

II. MODELS AND SUSY PARAMETERS

A. Models

In this section, we give a brief description of the models considered in this paper. They are well-motivated examples of SUSY models, and are chosen as representatives that have distinct flavor signals. Every model is reduced to the MSSM at low-energy scale, which is an $\mathrm{SU}(3)_C \times \mathrm{SU}(2)_L \times \mathrm{U}(1)_Y$ supersymmetric gauge theory with the SUSY being softly broken. The MSSM matter contents are the following chiral superfields:

$$\begin{aligned} &Q_i\left(3, 2, \frac{1}{6}\right), \qquad \bar{U}_i\left(\bar{3}, 1, -\frac{2}{3}\right), \qquad \bar{D}_i\left(\bar{3}, 1, \frac{1}{3}\right), \\ &L_i\left(1, 2, -\frac{1}{2}\right), \qquad \bar{E}_i(1, 1, 1), \qquad (i = 1, 2, 3) \\ &H_1\left(1, 2, -\frac{1}{2}\right), \qquad H_2\left(1, 2, \frac{1}{2}\right), \end{aligned} \tag{1}$$

where the gauge quantum numbers are shown in parentheses. The MSSM superpotential can be written as

$$\begin{aligned} \mathcal{W}_{\mathrm{MSSM}} = {} & y_D^{ij}\bar{D}_i Q_j H_1 + y_U^{ij}\bar{U}_i Q_j H_2 + y_E^{ij}\bar{E}_i L_j H_1 \\ & + \mu H_1 H_2, \end{aligned} \tag{2}$$

with an assumption of R-parity conservation and renormalizability. The SUSY breaking effect is described by the following soft SUSY breaking terms in the Lagrangian:

$$
\begin{aligned}
-\mathcal{L}_{\text{soft}}^{\text{MSSM}} &= (m_Q^2)^{ij}\tilde{q}_i^\dagger \tilde{q}_j + (m_U^2)^{ij}\tilde{u}_i^\dagger \tilde{u}_j + (m_D^2)^{ij}\tilde{d}_i^\dagger \tilde{d}_j \\
&+ (m_L^2)^{ij}\tilde{l}_i^\dagger \tilde{l}_j + (m_E^2)^{ij}\tilde{e}_i^\dagger \tilde{e}_j + m_{H_1}^2 h_1^\dagger h_1 \\
&+ m_{H_2}^2 h_2^\dagger h_2 - (B\mu h_1 h_2 + \text{H.c.}) \\
&+ (A_U^{ij}\tilde{u}_i^\dagger \tilde{q}_j h_2 + A_D^{ij}\tilde{d}_i^\dagger \tilde{q}_j h_1 + A_E^{ij}\tilde{e}_i^\dagger \tilde{l}_j h_1 \\
&+ \text{H.c.}) + \frac{M_3}{2}\tilde{\bar{g}}\,\tilde{g} + \frac{M_2}{2}\tilde{\bar{W}}\,\tilde{W} + \frac{M_1}{2}\tilde{\bar{B}}\,\tilde{B},
\end{aligned}
\tag{3}
$$

where $\tilde{q}_i$, $\tilde{u}_i^\dagger$, $\tilde{d}_i^\dagger$, $\tilde{l}_i$, $\tilde{e}_i^\dagger$, h_1, and h_2 are the corresponding scalar components of the chiral superfields given in Eq. (1), and $\tilde{g}$, $\tilde{W}$, and $\tilde{B}$ are $SU(3)_C$, $SU(2)_L$, and $U(1)_Y$ gauge fermions, respectively.

1. The minimal supergravity model

The mSUGRA consists of the MSSM sector and a hidden sector where the SUSY is assumed to be spontaneously broken. Only a gravitational interaction interconnects these two sectors. This gravitational interaction mediates the SUSY breaking effect from the hidden sector to the observable MSSM sector, and the soft breaking terms in Eq. (3) are induced in the following manner:

$$
\begin{aligned}
(m_Q^2)_{ij} &= (m_U^2)_{ij} = (m_D^2)_{ij} = (m_L^2)_{ij} = (m_E^2)_{ij} = m_0^2\delta_{ij}, \\
m_{H_1}^2 &= m_{H_2}^2 = m_0^2, \\
A_U^{ij} &= m_0 A_0 y_U^{ij}, \\
A_D^{ij} &= m_0 A_0 y_D^{ij}, \\
A_E^{ij} &= m_0 A_0 y_E^{ij}, \\
M_1 &= M_2 = M_3 = m_{1/2},
\end{aligned}
\tag{4}
$$

where we assume the GUT relation among the gaugino masses. The above relations are applied at the energy scale where the soft breaking terms are induced by the gravitational interaction. We identify this scale with the GUT scale ($\mu_G \simeq 2 \times 10^{16}$ GeV) for simplicity. Thus the soft breaking terms are specified at μ_G by the universal scalar mass, m_0, the universal gaugino mass, $m_{1/2}$, and the universal trilinear coupling, A_0. The soft breaking terms at the electroweak scale are determined by solving renormalization group equations.

In this model, the only source of flavor mixings is the CKM matrix. New flavor mixings in the squark sector at the electroweak scale come from the CKM matrix through radiative corrections [19,20]. In addition to the CP phase in the CKM matrix, there can be two physically independent CP phases. We take the complex phase of the μ term ($\phi_\mu \equiv \arg\mu$) and the phase of A_0 ($\phi_A \equiv \arg A_0$) as the new CP phases while we take the gaugino mass $m_{1/2}$ as real and positive by convention. These CP phases contribute to the neutron and electron electric dipole moments (EDMs) [9,30–33] and experimental constraints on these phases are very severe.

We assume that the generation mechanism of neutrino masses in this model does not affect the flavor mixing in the SUSY sector. For example, in the mSUGRA model with right-handed neutrinos, which is described below, the effect of the neutrino mass on the flavor mixing in the SUSY sector is negligible in a small right-handed neutrino mass limit.

2. The MSSM with right-handed neutrinos

Recent developments of neutrino experiments have established the existence of small finite masses of neutrinos. A simple extension of the mSUGRA model for giving small finite masses of neutrinos is introducing gauge singlet right-handed Majorana neutrino superfields, $\bar{N}_i$ ($i = 1, 2, 3$). This is known as the type I seesaw mechanism [34]. The superpotential can be written as

$$
\mathcal{W}_{\text{MSSM}\nu_R} = \mathcal{W}_{\text{MSSM}} + (y_N)^{ij}\bar{N}_i L_j H_2 + \frac{1}{2}(M_N)^{ij}\bar{N}_i\bar{N}_j,
\tag{5}
$$

which leads to the following higher dimensional term:

$$
\begin{aligned}
\Delta\mathcal{W}_\nu &= -\frac{1}{2}K_\nu^{ij}(L_i H_2)(L_j H_2), \\
K_\nu &= (y_N^T)^{ik}(M_N^{-1})^{kl}(y_N)^{lj},
\end{aligned}
\tag{6}
$$

after heavy fields $\bar{N}_{1,2,3}$ are integrated out at the energy scale below the Majorana mass scale ($\equiv \mu_R$). This higher dimensional term yields the neutrino mass matrix by the electroweak symmetry breaking as

$$
(m_\nu)^{ij} = (K_\nu)^{ij}\langle h_2\rangle^2.
\tag{7}
$$

Taking the basis in which the charged lepton mass matrix is diagonal, one can obtain the observable neutrino mass eigenvalues and the Pontecorvo-Maki-Nakagawa-Sakata (PMNS) mixing matrix [35] as

$$
(m_\nu)^{ij} = (V_{\text{PMNS}}^*)^{ik} m_{\nu_k} (V_{\text{PMNS}}^\dagger)^{kj}.
\tag{8}
$$

From the neutrino oscillation experiments, it is known that there is a hierarchy among the two squared mass differences as $|m_{\nu_3}^2 - m_{\nu_2}^2| \gg |m_{\nu_2}^2 - m_{\nu_1}^2|$. We define ν_1 and ν_2 so that $m_{\nu_2} > m_{\nu_1}$. Therefore there are two possibilities for the neutrino mass hierarchy when the mass of the lightest neutrino is much smaller than the mass splittings.

(i) Normal hierarchy: $m_{\nu_3} \gg m_{\nu_2} > m_{\nu_1}$;
(ii) Inverted hierarchy: $m_{\nu_2} > m_{\nu_1} \gg m_{\nu_3}$.

When the overall mass scale is much larger than the mass splittings, all the three neutrinos are nearly degenerate in mass. In the present analysis we take

(iii) Degenerate: $m_{\nu_3} \gtrsim m_{\nu_2} \gtrsim m_{\nu_1}$.

For numerical calculations, we consider three sets of low-energy neutrino parameters corresponding to the above three cases.

As for the soft breaking terms, scalar mass terms, A terms, and B terms of sneutrinos, $\tilde{\nu}_i^\dagger$, are added as

$$-\mathcal{L}_{\rm soft}^{\rm MSSM\nu_R} = -\mathcal{L}_{\rm soft}^{\rm MSSM} + (m_N^2)^{ij}\tilde{\nu}_i^\dagger\tilde{\nu}_j + (A_N^{ij}\tilde{\nu}_i\tilde{l}_j h_2 + (\tilde{m}_N^2)^{ij}\tilde{\nu}_i^\dagger\tilde{\nu}_j^\dagger + \text{H.c.}). \quad (9)$$

We assume that the soft breaking terms are generated in a universal fashion at μ_G, i.e.,

$$(m_N^2)^{ij} = m_0^2\delta^{ij}, \qquad A_N^{ij} = m_0 A_0 y_N^{ij}. \quad (10)$$

We neglect the $\tilde{m}_N^2$ terms in the present work. These terms can significantly affect the EDMs, while contributions to the lepton flavor violation processes are subdominant [36].

The new flavor mixing in the scalar lepton sector comes from the neutrino mixing through the renormalization group running between μ_G and μ_R. In the leading logarithmic approximation, they are given as

$$(m_L^2)^{ij} \simeq -\frac{1}{8\pi^2}m_0^2(3+|A_0|^2)(y_N^\dagger y_N)^{ij}\ln\frac{\mu_G}{\mu_R}, \quad (11a)$$

$$(m_E^2)^{ij} \simeq 0, \quad (11b)$$

$$(A_E)^{ij} \simeq -\frac{3}{8\pi^2}m_0 A_0 y_e^i(y_N^\dagger y_N)^{ij}\ln\frac{\mu_G}{\mu_R}, \quad (11c)$$

for $i \neq j$. We numerically solve full RGEs in the actual analysis given in Sec. III. Consequences of these mixings on lepton flavor violating processes have been investigated from various aspects. Lepton flavor violating processes such as $\mu \to e\gamma$ are sensitive to the off-diagonal elements of $y_N^\dagger y_N$ [37].

As we have discussed in the end of the last subsection, this model reduces to the mSUGRA model in the limit of $y_N \to 0$. For instance, the effect of (11) is negligible if $\mu_R \ll 10^{12}$ GeV.

We consider three typical structures of the neutrino Yukawa couplings.

(i) degenerate ν_R case

$$y_N = \frac{\sqrt{\hat{M}_N}}{\langle h_2\rangle}\begin{pmatrix}\sqrt{m_{\nu_1}} & 0 & 0\\ 0 & \sqrt{m_{\nu_2}} & 0\\ 0 & 0 & \sqrt{m_{\nu_3}}\end{pmatrix}V_{\rm PMNS}^\dagger. \quad (12)$$

This is a case that all the masses of the right-handed neutrinos are the same and there are no CP phases in the heavy neutrino sector. In Eq. (12), $\hat{M}_N$ denotes the eigenvalue of the right-handed neutrino mass matrix, i.e, $(M_N)^{ij} = \hat{M}_N\delta^{ij}$. In this simplest case, the mixing in y_N should be identified with the PMNS mixing because there is no flavor structure in M_N. The large mixing in the PMNS matrix leads to large off-diagonal elements of $y_N^\dagger y_N$, which enhance the $\mu \to e\gamma$ branching ratio. As we will see later, the SUSY breaking parameter space is strongly constrained by the present experimental limit in the normal hierarchy case.

(ii) nondegenerate ν_R (I)

$$y_N = \begin{pmatrix}y_{11} & 0 & 0\\ 0 & y_{22} & y_{23}\\ 0 & y_{32} & y_{33}\end{pmatrix}. \quad (13)$$

In this case, the PMNS mixing arises from the above y_N and a nondegenerate mass matrix of right-handed neutrinos, M_N, as is described in Sec. III B. Because $y_N^\dagger y_N$ has the same texture as y_N in Eq. (13), $\mu \to e\gamma$ is suppressed enough to satisfy the present experimental bound. As for other LFV processes, $\tau \to e\gamma$ is also suppressed, while $\tau \to \mu\gamma$ is not. The specific structure in Eq. (13) could be an implication of electron-number conservation which works above the right-handed neutrino mass scale, μ_R, and is broken by the right-handed neutrino mass matrix, M_N.

(iii) nondegenerate ν_R (II)

$$y_N = \begin{pmatrix}y_{11} & 0 & y_{13}\\ 0 & y_{22} & 0\\ y_{31} & 0 & y_{33}\end{pmatrix}. \quad (14)$$

This case is similar to the nondegenerate ν_R (I) case, except that the first and the second generations are interchanged in y_N. Accordingly, $\mu \to e\gamma$ and $\tau \to \mu\gamma$ are suppressed, while we expect a larger branching ratio of $\tau \to e\gamma$.

3. The SU(5) SUSY GUT with right-handed neutrinos

The idea of supersymmetric grand unification is supported by the precise determination of three gauge coupling constants at LEP and other experiments in the last decade. In view of this, we consider SU(5) SUSY GUT with right-handed neutrinos as an extension of the MSSM with right-handed neutrinos. Here we follow the analysis of Refs. [23,27] and we give a brief description of the model.

This model is defined by the following superpotential:

$$\mathcal{W}_{\rm SU(5)\nu_R} = \frac{1}{8}\epsilon_{abcde}(\lambda_U)^{ij}(T_i)^{ab}(T_j)^{cd}H^e + (\lambda_D)^{ij}(\bar{F}_i)_a(T_j)^{ab}\bar{H}_b + (\lambda_N)^{ij}\bar{N}_i(\bar{F}_j)_a H^a + \frac{1}{2}(M_N)^{ij}\bar{N}_i\bar{N}_j + \mathcal{W}_H + \Delta\mathcal{W}_{\rm SU(5)\nu_R}, \quad (15)$$

where i and j are generation indexes, while a, b, c, d, and e are SU(5) indices. ϵ_{abcde} denotes the totally antisymmetric tensor of the SU(5). T_i, $\bar{F}_i$, and $\bar{N}_i$ are **10**, $\bar{\mathbf{5}}$, and **1** representations of the SU(5) gauge group, respectively. Q_i, $\bar{U}_i$, and $\bar{E}_i$ are embedded in T_i, $\bar{F}_i$ consists of $\bar{D}_i$ and L_i, and $\bar{N}_i$ is identified with the right-handed heavy Majorana neutrinos. H ($\bar{H}$) denotes a Higgs superfield in **5** ($\bar{\mathbf{5}}$) representation and includes $H_C(\mathbf{3},\mathbf{1},-\frac{1}{3})$ and H_2 ($\bar{H}_C(\bar{\mathbf{3}},\mathbf{1},\frac{1}{3})$ and H_1). $(\lambda_U)^{ij}$, $(\lambda_D)^{ij}$, and $(\lambda_N)^{ij}$ are the Yukawa coupling matrices, and $(M_N)^{ij}$ is the Majorana mass matrix. The superpotential for Higgs superfields, $\mathcal{W}_H$, contains terms with H, $\bar{H}$, and Σ_b^a which is a **24**

representation of the SU(5) gauge group. It is assumed that a vacuum expectation value (VEV) of $\Sigma^a{}_b$, $\langle\Sigma^a{}_b\rangle = \mathrm{diag}(\frac{1}{3},\frac{1}{3},\frac{1}{3},-\frac{1}{2},-\frac{1}{2})v_G$ breaks the SU(5) symmetry to $\mathrm{SU}(3)_C \times \mathrm{SU}(2)_L \times \mathrm{U}(1)_Y$ at μ_G. $\Delta\mathcal{W}_{\mathrm{SU}(5)\nu_R}$ is a dimension-five operator, which is introduced in order to reproduce the realistic mass relations between the down-type quarks and charged leptons, as explained in Ref. [27].

The supermultiplets with the masses of order of the GUT scale such as H_C and $\bar{H}_C$ are integrated out at μ_G and the effective theory below μ_G is the MSSM with the right-handed neutrinos described by the superpotential $\mathcal{W}_{\mathrm{MSSM}\nu_R}$ in Eq. (6). The Yukawa coupling matrices in Eq. (6) are related to those in Eq. (15) as $(y_U)^{ij} = (\lambda_U)^{ij}$ and $(y_N)^{ij} = (\lambda_N)^{ij}$. $(\lambda_D)^{ij}$ is determined from $(y_D)^{ij}$ and $(y_E)^{ij}$, taking $O(\mu_G/\mu_P)$ corrections from $\Delta\mathcal{W}_{\mathrm{SU}(5)\nu_R}$ into account [27].

There are additional degrees of freedom in the matching relations between $y_{U,D,E,N}$ and $\lambda_{U,D,N}$, which cannot be determined from the quark and lepton masses and the CKM and PMNS matrices at low energy [23,24,38]. In the present analysis, we introduce only two relative phase parameters for simplicity, which correspond to $\hat{\Theta}_L$ in Ref. [24].

The SU(5) invariant and renormalizable soft breaking terms are written as

$$
\begin{aligned}
-\mathcal{L}^{\mathrm{SU}(5)}_{\mathrm{soft}} &= \frac{1}{2}(m^2_T)^{ij}(\tilde{T}^*_i)_{ab}(\tilde{T}_j)^{ab} + (m^2_{\tilde{F}})^{ij}(\tilde{\bar{F}}^*_i)^a(\tilde{\bar{F}}_j)_a + (m^2_{\tilde{N}})^{ij}\tilde{\bar{N}}^*_i\tilde{\bar{N}}_j + (m^2_H)H^*{}_aH^a + (m^2_{\bar{H}})\bar{H}^{*a}\bar{H}_a \\
&\quad + \left(\frac{3}{2}B_H\lambda_H v_G\bar{H}_aH^a + \mathrm{H.c.}\right) + (\text{terms with } \Sigma^a{}_b) + \left\{\frac{1}{8}\epsilon_{abcde}(\tilde{\lambda}_U)^{ij}(\tilde{T}_i)^{ab}(\tilde{T}_j)^{cd}H^e + (\tilde{\lambda}_D)^{ij}(\tilde{\bar{F}}_i)_a(\tilde{T}_j)^{ab}\bar{H}_b\right. \\
&\quad \left. + (\tilde{\lambda}_N)^{ij}\tilde{\bar{N}}_i(\tilde{\bar{F}}_j)_aH^a + \frac{1}{2}(\tilde{M}_N)^{ij}\tilde{\bar{N}}_i\tilde{\bar{N}}_j + \mathrm{H.c.}\right\} + \frac{1}{2}M_5\tilde{\bar{G}}_5\tilde{G}_5, \qquad (16)
\end{aligned}
$$

where $\tilde{T}_i$, $\tilde{\bar{F}}_i$, and $\tilde{\bar{N}}_i$ are the scalar components of T_i, $\bar{F}_i$, and $\bar{N}_i$, respectively; H and $\bar{H}$ stand for the corresponding scalar components of the superfields denoted by the same symbols; and $\tilde{G}_5$ represents the SU(5) gaugino. We assume that the soft breaking terms are generated in a universal fashion at the Planck scale, μ_P, i.e.,

$$
(m^2_T)^{ij} = (m^2_{\bar{F}})^{ij} = (m^2_{\bar{N}})^{ij} = m_0^2\delta^{ij}, \qquad (\tilde{\lambda})^{ij} = m_0A_0(\lambda)^{ij}, \qquad (\lambda = \lambda_U, \lambda_D, \lambda_N), \qquad M_5 = m_{1/2}. \qquad (17)
$$

We solve the RG equations of the SU(5) SUSY GUT from μ_P to μ_G with Eq. (17) as boundary conditions at μ_P, then those of MSSM with right-handed neutrinos between the μ_G and μ_R. Finally, the squark and slepton mass matrices are obtained by the RG equations of the MSSM below μ_R.

Unlike the previous two models, a large flavor mixing in the neutrino sector can affect the right-handed down-type squark sector because the lepton doublets and the down quarks are embedded in the same representation of SU(5). For a similar reason, the CKM mixing in the quark sector contributes to the mixing in the right-handed charged slepton sector [20,21]. For instance, the correction to $m^2_{\tilde{E}}$ is given in the leading logarithmic approximation as

$$
(m^2_{\tilde{E}})^{ij} \simeq -\frac{3}{8\pi^2}m_0^2(3 + |A_0|^2)(\lambda^\dagger_U\lambda_U)^{ij}\ln\frac{\mu_P}{\mu_G}. \qquad (18)
$$

Quark flavor signals in models with a grand unification have been studied in literature [23–25]. It is shown in these papers that large contributions to ϵ_K and the $\mu \to e\gamma$ decay can arise from the new source of flavor mixing in the neutrino sector.

We study the same patterns of neutrino Yukawa couplings as those in MSSM with right-handed neutrinos, i.e., degenerate ν_R, nondegenerate ν_R (I), and nondegenerate ν_R (II) cases.

4. A model with U(2) flavor symmetry

There is a class of models which are intended to solve the flavor problem of the MSSM by introducing appropriate symmetry structure. U(2) flavor symmetry [39,40] is a typical example of such models. We consider the model given in Ref. [40]. In this model, the quark and lepton supermultiplets in the first and the second generations transform as doublets under the U(2) flavor symmetry, and the third generation and the Higgs supermultiplets are singlets under the U(2). In addition to the ordinary matter fields, we introduce the following superfields: a doublet $\Phi^i(-1)$, a symmetric tensor $S^{ij}(-2)$, and an anti-symmetric tensor $A^{ij}(-2)$, where i and j run over the first two generations and the numbers in the parentheses represent the charge of the U(1) subgroup.

The U(2) invariant superpotential relevant to the quark Yukawa couplings is given as follows:

$$
\begin{aligned}
\mathcal{W}_{\mathrm{U}(2)} &= Y_U\left(\bar{U}_3Q_3H_2 + \frac{b_U}{M_F}\Phi^i\bar{U}_iQ_3H_2 + \frac{c_U}{M_F}\bar{U}_3\Phi^iQ_iH_2 + \frac{d_U}{M_F}S^{ij}\bar{U}_iQ_jH_2 + \frac{a_U}{M_F}A^{ij}\bar{U}_iQ_jH_2\right) \\
&\quad + Y_D\left(\bar{D}_3Q_3H_1 + \frac{b_D}{M_F}\Phi^i\bar{D}_iQ_3H_1 + \frac{c_D}{M_F}\bar{D}_3\Phi^iQ_iH_1 + \frac{d_D}{M_F}S^{ij}\bar{D}_iQ_jH_1 + \frac{a_D}{M_F}A^{ij}\bar{D}_iQ_jH_1\right), \qquad (19)
\end{aligned}
$$

where M_F is the scale of the flavor symmetry, and Y_Q, a_Q, b_Q, c_Q, and d_Q ($Q = U, D$) are dimensionless coupling constants. Dimension-five and higher dimensional operators are neglected in the superpotential in Eq. (19). Absolute values of the above dimensionless coupling constants except for Y_D are supposed to be of $O(1)$.

The breaking pattern of the U(2) symmetry is assumed to be

$$\mathrm{U}(2) \longrightarrow \mathrm{U}(1) \longrightarrow \text{no symmetry}, \tag{20}$$

in order to reproduce the preferable quark Yukawa coupling matrices which can explain the mass eigenvalues and the mixing of quarks. The first breaking is induced by VEV's of Φ^i and S^{ij}, and the second one by a VEV of A^{ij}. These VEV's are given as

$$\frac{\langle \Phi^i \rangle}{M_F} = \delta^{i2}\epsilon, \qquad \frac{\langle S^{ij} \rangle}{M_F} = \delta^{i2}\delta^{j2}\epsilon, \qquad \frac{\langle A^{ij} \rangle}{M_F} = \epsilon^{ij}\epsilon', \tag{21}$$

where ϵ and ϵ' are taken to be real without loss of generality. Because ϵ and ϵ' are order parameters of the U(2) and U(1) symmetry breaking, respectively, they satisfy $\epsilon' \ll \epsilon$. Note that $\langle S^{ij} \rangle$ is chosen to leave the U(1) unbroken. With the breaking pattern given in Eq. (20), we obtain the quark Yukawa coupling matrix y_Q as

$$y_Q^{ij} = Y_Q \begin{pmatrix} 0 & a_Q\epsilon' & 0 \\ -a_Q\epsilon' & d_Q\epsilon & b_Q\epsilon \\ 0 & c_Q\epsilon & 1 \end{pmatrix}, \qquad Q = U, D. \tag{22}$$

The U(2) symmetry controls not only the superpotential but also the soft breaking terms. After the U(2) broken with the pattern in Eq. (20), the squark mass matrices m_X^2 can be obtained as

$$m_X^2 = (m_0^X)^2 \begin{pmatrix} 1 & 0 & 0 \\ 0 & 1 + r_{22}^X\epsilon^2 & r_{23}^X\epsilon \\ 0 & r_{23}^{X*}\epsilon & r_{33}^X \end{pmatrix}, \qquad X = Q, U, D, \tag{23}$$

where r_{ij}^X are dimensionless parameters of $O(1)$. As for the squark A terms, they have the same structure as the quark Yukawa coupling matrices:

$$A_Q^{ij} = A_Q^0 Y_Q \begin{pmatrix} 0 & \tilde{a}_Q\epsilon' & 0 \\ -\tilde{a}_Q\epsilon' & \tilde{d}_Q\epsilon & \tilde{b}_Q\epsilon \\ 0 & \tilde{c}_Q\epsilon & 1 \end{pmatrix}, \qquad Q = U, D. \tag{24}$$

In general, though being of $O(1)$, $\tilde{a}_Q$, $\tilde{b}_Q$, $\tilde{c}_Q$, and $\tilde{d}_Q$ take different values from the corresponding parameters in Eq. (22), and we expect no exact universality of the A terms in this model.

With the help of the U(2) symmetry, the masses of the first- and second-generation squarks are naturally degenerate. On the other hand, the mass of the third-generation squarks may be separated from the others. There exist flavor mixings of $O(\epsilon)$ between the second and the third generations of squarks. These are new sources of flavor mixing besides the CKM matrix.

There are several efforts to explain the observed neutrino masses and mixings in SUSY models with the U(2) flavor symmetry (or its discrete relatives) [41]. Unlike the quark sector, application of the U(2) symmetry to the lepton sector is not straightforward because of the large mixings of the neutrinos. Therefore we focus on the quark sector in the following analysis, taking the same boundary conditions as Eq. (4) for the slepton sector.

B. Treatments of radiative breaking of the electroweak symmetry

In the models we consider, SUSY parameters such as m_0, $m_{1/2}$, A_0, etc. are given at the high-energy cutoff scale. In order to analyze flavor signals, we need to connect the parameters at the cutoff scale and those at the electroweak scale with help of the renormalization group equations. In the present work, we adopt the following procedure to determine the parameters at the electroweak scale.

(1) The masses of quarks and leptons and the mixings (the CKM and PMNS matrices) are given as inputs at the electroweak scale, $\mu_W = M_Z$. These masses are running masses in the standard model. The Yukawa couplings and the coupling matrix of the dimension-five operator K_ν in Eq. (6) are determined by these masses and another input parameter, $\tan\beta \equiv \langle h_2 \rangle / \langle h_1 \rangle$.

(2) Two-loop RGEs for the Yukawa couplings and K_ν, as well as the gauge coupling constants, are solved up to a high-energy cutoff scale with the boundary conditions given at μ_W. The cutoff scale is taken as the GUT scale, μ_G, for the mSUGRA, the MSSM with right-handed neutrinos, and the U(2) model and the Planck scale, μ_P, for the SU(5) SUSY GUT with right-handed neutrinos. By this procedure, we calculate the parameters in the superpotential at the cutoff scale. A schematic picture of the cutoff scale involved in these models is displayed in Fig. 1. Here, the $\overline{\mathrm{DR}}'$ scheme [42] is adopted as a renormalization scheme.

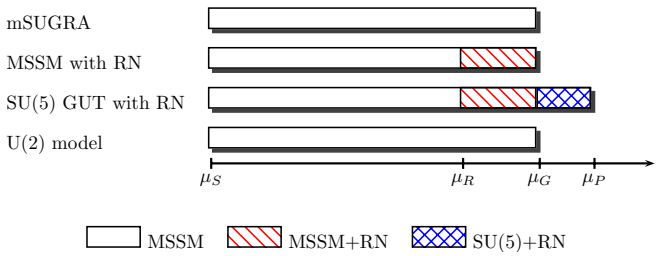

FIG. 1 (color online). The cutoff scales and the models. RN stands for right-handed neutrinos.

In the MSSM with right-handed neutrinos and SU(5) SUSY GUT with right-handed neutrinos, we decompose K_ν to y_N and M_N at the μ_R scale so that they satisfy the seesaw relation, Eq. (6). In the SU(5) SUSY GUT with right-handed neutrinos the parameters in $\mathcal{W}_{\mathrm{SU}(5)\nu_R}$ are matched with the MSSM with right-handed neutrinos at the GUT scale, μ_G.

(3) The boundary conditions for the soft SUSY breaking parameters are set at the cutoff scale as Eq. (4) for the mSUGRA, Eq. (4) and (10) for the MSSM with right-handed neutrinos, Eq. (17) for the SU(5) SUSY GUT with right-handed neutrinos, and Eq. (23) for the U(2) model. We take the same boundary conditions for the A parameters in the U(2) model as the mSUGRA case for simplicity.

(4) With help of two-loop RGEs, we evaluate the soft breaking terms at a typical SUSY breaking scale, $\mu_S = 1$ TeV, and calculate the SUSY masses and mixings at the leading order which are considered as $\overline{\mathrm{DR}}'$ masses. For the masses of the Higgs bosons, the one-loop corrections are included.
Then we set the value of μ and B so that the tadpole diagrams of the Higgs bosons up to one-loop level vanish.
Then running the μ to the electroweak scale M_Z, we obtain the μ at M_Z.

(5) The SUSY threshold corrections to the gauge couplings and the masses of quarks and leptons are evaluated in order to determine $\overline{\mathrm{DR}}'$ gauge couplings, $\overline{\mathrm{DR}}'$ Higgs VEV, and $\overline{\mathrm{DR}}'$ masses of the matter fermions in the MSSM which lead to the $\overline{\mathrm{DR}}'$ Yukawa couplings, according to Ref. [43].

(6) We iterate from two to five in the above list until the numerical behavior converges.

(7) The physical mass spectrum of SUSY particles is calculated at the M_Z scale up to one-loop level [43]. The flavor observables are also calculated with the parameters determined at the M_Z scale.

In comparison with the previous work, two-loop RGEs for the running of SUSY parameters are used and the one-loop SUSY threshold corrections at the electroweak scale are included in the calculation of this work.

III. NUMERICAL ANALYSIS

A. Flavor observables

The flavor observables considered in the following are the $K^0 - \bar{K}^0$, $B_d - \bar{B}_d$, and $B_s - \bar{B}_s$ mixings, both the direct and mixing-induced CP asymmetries of $b \to s\gamma$ and $b \to d\gamma$, and the time-dependent CP asymmetry of $B \to \phi K_S$. The branching ratios of the lepton flavor violating decay processes $\mu \to e\gamma$, $\tau \to \mu\gamma$, and $\tau \to e\gamma$ are also evaluated in the MSSM with right-handed neutrinos and SU(5) SUSY GUT with right-handed neutrinos. As mentioned in Sec. II A 4, we do not consider the flavor signals in the lepton sector for the U(2) model. Here we show the calculation methods of the flavor observables briefly. Detail on the calculation methods of the flavor observables is available in Refs. [23,27,28].

1. $K - \bar{K}$ and $B - \bar{B}$ mixings

The $K^0 - \bar{K}^0$, $B_d - \bar{B}_d$, and $B_s - \bar{B}_s$ mixings are described by the effective Lagrangian of the following form:

$$\begin{aligned}\mathcal{L}_{\Delta F=2} = {} & C_{LL}(\bar{q}_L^\alpha \gamma^\mu Q_{L\alpha})(\bar{q}_L^\beta \gamma_\mu Q_{L\beta}) + C_{RR}(\bar{q}_R^\alpha \gamma^\mu Q_{R\alpha}) \\ & \times (\bar{q}_R^\beta \gamma_\mu Q_{R\beta}) + C_{LR}^{(1)}(\bar{q}_R^\alpha Q_{L\alpha})(\bar{q}_L^\beta Q_{R\beta}) \\ & + C_{LR}^{(2)}(\bar{q}_R^\alpha Q_{L\beta})(\bar{q}_L^\beta Q_{R\alpha}) + \tilde{C}_{LL}^{(1)}(\bar{q}_R^\alpha Q_{L\alpha})(\bar{q}_R^\beta Q_{L\beta}) \\ & + \tilde{C}_{LL}^{(2)}(\bar{q}_R^\alpha Q_{L\beta})(\bar{q}_R^\beta Q_{L\alpha}) + \tilde{C}_{RR}^{(1)}(\bar{q}_L^\alpha Q_{R\alpha})(\bar{q}_L^\beta Q_{R\beta}) \\ & + \tilde{C}_{RR}^{(2)}(\bar{q}_L^\alpha Q_{R\beta})(\bar{q}_L^\beta Q_{R\alpha}), \end{aligned} \tag{25}$$

where $(q, Q) = (d, b)$, (s, b), and (d, s) for the $B_d - \bar{B}_d$, $B_s - \bar{B}_s$, and $K^0 - \bar{K}^0$ mixings, respectively, and the suffixes α and β denote color indices. New physics contributions to the Wilson coefficients C's, as well as the SM ones, are obtained by calculating relevant box diagrams. Explicit formulae of the coefficients are found in, e.g., Ref. [23]. The mixing matrix elements $M_{12}(B_d)$, $M_{12}(B_s)$, and $M_{12}(K)$ are given as

$$M_{12}(P) = -\frac{1}{2m_P}\langle P|\mathcal{L}_{\Delta F=2}|\bar{P}\rangle, \tag{26}$$

where $P = B_d, B_s, K^0$.

In the evaluation of the matrix elements $\langle P|\mathcal{L}_{\Delta F=2}|\bar{P}\rangle$, we parametrize the matrix elements of the operators in Eq. (25) as

$$\langle K^0|(\bar{d}_L^\alpha \gamma^\mu s_{L\alpha})(\bar{d}_L^\beta \gamma_\mu s_{L\beta})|\bar{K}^0\rangle = \frac{2}{3} m_K^2 f_K^2 B_K, \tag{27a}$$

$$\langle K^0|(\bar{d}_R^\alpha s_{L\alpha})(\bar{d}_L^\beta s_{R\beta})|\bar{K}^0\rangle = \frac{1}{2}\left(\frac{m_K}{m_s + m_d}\right)^2 m_K^2 f_K^2 B_K^{LR(1)}, \tag{27b}$$

$$\langle K^0|(\bar{d}_R^\alpha s_{L\beta})(\bar{d}_L^\beta s_{R\alpha})|\bar{K}^0\rangle = \frac{1}{6}\left(\frac{m_K}{m_s + m_d}\right)^2 m_K^2 f_K^2 B_K^{LR(2)}, \tag{27c}$$

$$\langle K^0|(\bar{d}_L^\alpha s_{R\alpha})(\bar{d}_L^\beta s_{R\beta})|\bar{K}^0\rangle = -\frac{5}{12}\left(\frac{m_K}{m_s + m_d}\right)^2 m_K^2 f_K^2 \tilde{B}_K^{RR(1)}, \tag{27d}$$

$$\langle K^0|(\bar{d}_L^\alpha s_{R\beta})(\bar{d}_L^\beta s_{R\alpha})|\bar{K}^0\rangle = \frac{1}{12}\left(\frac{m_K}{m_s + m_d}\right)^2 m_K^2 f_K^2 \tilde{B}_K^{RR(2)}, \tag{27e}$$

where B_K, $B_K^{LR(1,2)}$, and $\tilde{B}_K^{RR(1,2)}$ are bag parameters. $B-\bar{B}$ mixing matrix elements are also defined in the same way. The bag parameters of B and K mesons and the decay constants of the B mesons are evaluated by the lattice QCD method [44]. We list the numerical values used in our calculation in Table I.

The observables ε_K, Δm_{B_d}, and Δm_{B_s} are expressed in terms of M_{12} as

$$\varepsilon_K = \frac{e^{i\pi/4}\,\mathrm{Im}M_{12}(K)}{\sqrt{2}\Delta m_K}, \tag{28}$$

$$\Delta m_{B_d} = 2|M_{12}(B_d)|, \tag{29}$$

$$\Delta m_{B_s} = 2|M_{12}(B_s)|. \tag{30}$$

2. CP asymmetries in B meson decays

The time-dependent CP asymmetry in the B_d decays to a CP eigenstate f_{CP} given by

$$\frac{\Gamma(\bar{B}_d(t)\to f_{CP})-\Gamma(B_d(t)\to f_{CP})}{\Gamma(\bar{B}_d(t)\to f_{CP})+\Gamma(B_d(t)\to f_{CP})} = A_{CP}(B_d\to f_{CP})\cos\Delta m_{B_d}t + S_{CP}(B_d\to f_{CP})\sin\Delta m_{B_d}t, \tag{31}$$

where A_{CP} and S_{CP} are direct and indirect (mixing-induced) CP violation parameters, respectively.

For $f_{CP}=J/\psi K_S$, the $b\to c\bar{c}s$ decay amplitude is assumed to be dominated by the tree-level standard model contribution. Consequently, the direct CP asymmetry $A_{CP}(B_d\to J/\psi K_S)$ is negligibly small. The weak phase of the $b\to c\bar{c}s$ decay amplitude comes from a product of the CKM matrix elements $V_{cb}V_{cs}^*$, which is almost real by convention. Therefore we can write

$$\frac{\Gamma(\bar{B}_d(t)\to J/\psi K_S)-\Gamma(B_d(t)\to J/\psi K_S)}{\Gamma(\bar{B}_d(t)\to J/\psi K_S)+\Gamma(B_d(t)\to J/\psi K_S)} = S_{CP}(B_d\to J/\psi K_S)\sin\Delta m_{B_d}t, \tag{32}$$

$$S_{CP}(B_d\to J/\psi K_S) = \sin\phi_M, \tag{33}$$

with ϕ_M being $e^{i\phi_M}=M_{12}(B_d)/|M_{12}(B_d)|$. In the standard model, $\phi_M=2\phi_1=2\arg(-V_{cb}^*V_{cd}/(V_{tb}^*V_{td}))$. Experimentally, $\sin\phi_M$ can be determined by combining decay modes with the $b\to c\bar{c}s$ transition such as $B_d\to J/\psi K_S$, $B_d\to J/\psi K_L$, and $B_d\to\psi' K_S$.

TABLE I. Decay constants and bag parameters for the $B^0-\bar{B}^0$ and the $K^0-\bar{K}^0$ mixing matrix elements [44] used in the numerical calculation. Here f_K is the experimental value.

P	f_P (MeV)	B_P	$B_P^{LR(1)}$	$B_P^{LR(2)}$	$\tilde{B}_P^{RR(1)}$	$\tilde{B}_P^{RR(2)}$
K	159.8	0.63	1.03	0.77	0.59	0.85
B_d	198	0.87	1.15	1.72	0.79	0.92
B_s	239	0.87	1.16	1.75	0.80	0.94

The time-dependent CP asymmetry in the B_s decay is formulated in the same way. $B_s\to J/\psi\phi$ is the $b\to c\bar{c}s$ mode of the B_s decay, which corresponds to $B_d\to J/\psi K_S$. The mixing-induced CP violation parameter $S_{CP}(B_s\to J/\psi\phi)$ is written as $S_{CP}(B_s\to J/\psi\phi)=\sin\phi_{M_s}$ where ϕ_{M_s} is defined as $e^{i\phi_{M_s}}=M_{12}(B_s)/|M_{12}(B_s)|$. In actual extraction, the angular analysis is needed to separate CP odd and even contribution [12,45]. The standard model prediction is given as $\sin\phi_{M_s}|_{\mathrm{SM}}\simeq -0.04$.

We also consider the decay mode $B_d\to\phi K_S$, which is supposed to be a pure $b\to s\bar{s}s$ process. The mixing-induced CP asymmetry $S_{CP}(B_d\to\phi K_S)$, is given as

$$S_{CP}(B_d\to\phi K_S) = \frac{2\,\mathrm{Im}(e^{-i\phi_M}\bar{\mathcal{A}}\mathcal{A})}{|\mathcal{A}|^2+|\bar{\mathcal{A}}|^2}, \tag{34}$$

where $\mathcal{A}$ and $\bar{\mathcal{A}}$ denote decay amplitudes of $B_d\to\phi K$ and $\bar{B}_d\to\phi\bar{K}$, respectively. This quantity is expected to coincide with $S_{CP}(B_d\to J/\psi K_S)$ within the SM. If there is sizable deviation, this will be an evidence of new physics beyond the SM in $b\to s$ transition. The calculation of the decay amplitude involves sizable uncertainty. Here we use a method based on the naive factorization. Details of the calculation of $\mathcal{A}$ are given in Refs. [24,46].

As for the $b\to q\gamma$ ($q=s,d$) decays, both direct and mixing-induced CP asymmetries are considered, as well as the branching ratio $\mathrm{B}(b\to s\gamma)$, which provides a significant constraint on the parameter space. Relevant effective Lagrangian is given as

$$\mathcal{L} = C_{2L}\mathcal{O}_{2L}+C'_{2L}\mathcal{O}'_{2L}-C_{7L}\mathcal{O}_{7L}-C_{8L}\mathcal{O}_{8L} + (L\leftrightarrow R)+\mathcal{L}_{4q}. \tag{35}$$

The operators $\mathcal{O}$'s are

$$\mathcal{O}_{2L} = (\bar{q}_\alpha\gamma^\mu c_{L\alpha})(\bar{c}_\beta\gamma^\mu b_{L\beta}), \tag{36a}$$

$$\mathcal{O}'_{2L} = (\bar{q}_\alpha\gamma^\mu u_{L\alpha})(\bar{u}_\beta\gamma^\mu b_{L\beta})-(\bar{q}_\alpha\gamma^\mu c_{L\alpha})(\bar{c}_\beta\gamma^\mu b_{L\beta}), \tag{36b}$$

$$\mathcal{O}_{7L} = \frac{e}{16\pi^2}m_b\bar{q}\frac{i}{2}[\gamma^\mu,\gamma^\nu]b_R F_{\mu\nu}, \tag{36c}$$

$$\mathcal{O}_{8L} = \frac{g_3}{16\pi^2}m_b\bar{q}^\alpha\frac{i}{2}[\gamma^\mu,\gamma^\nu]T^{(a)}_{\alpha\beta}b_R^\beta G^{(a)}_{\mu\nu}, \tag{36d}$$

where q is s or d for $b\to s\gamma$ or $b\to d\gamma$ decays, respectively. $\mathcal{L}_{4q}$ denotes the terms with four-quark operators induced by loop effects. The Wilson coefficients C_{2L} and C'_{2L} are dominated by the contributions from the tree-level W boson exchange. Therefore, $C'_{2L}=\epsilon_u C_{2L}$ is satisfied, where $\epsilon_u=-V_{uq}^*V_{ub}/(V_{tq}^*V_{tb})$. The direct CP asymmetry in the inclusive decays $B\to X_q\gamma$ ($q=s,d$) is given as [47]

$$A_{CP}^{\rm dir}(B\to X_q\gamma)=\frac{\Gamma(\bar B\to X_q\gamma)-\Gamma(B\to X_{\bar q}\gamma)}{\Gamma(\bar B\to X_q\gamma)+\Gamma(B\to X_{\bar q}\gamma)}$$
$$=-\frac{\alpha_3}{\pi(|C_{7L}|^2+|C_{7R}|^2)}$$
$$\times\Big[-{\rm Im}r_2{\rm Im}[(1-\epsilon_u)C_{2L}C_{7L}^*]$$
$$+\frac{80}{81}\pi{\rm Im}(\epsilon_u C_{2L}C_{7L}^*)+\frac{8}{9}\pi{\rm Im}(C_{8L}C_{7L}^*)$$
$$-{\rm Im}f_{27}{\rm Im}[(1-\epsilon_u)C_{2L}C_{7L}^*]$$
$$+\frac{1}{3}{\rm Im}f_{27}{\rm Im}[(1-\epsilon_u)C_{2L}C_{8L}^*]+(L\leftrightarrow R)\Big], \quad (37)$$

where the functions r_2 and f_{27} for $B\to X_s\gamma$ are found in Ref. [48]. The mixing-induced CP asymmetry is defined for an exclusive $B_d\to M_q\gamma$ decay. M_q denotes a hadronic CP eigenstate which includes a strange or down quark such as K^* (for $q=s$) and ρ ($q=d$). $S_{CP}(B_d\to M_q\gamma)$ is given as [49]

$$S_{CP}(B_d\to M_q\gamma)=\frac{2\,{\rm Im}(e^{-i\phi_M}C_{7L}C_{7R})}{|C_{7L}|^2+|C_{7R}|^2}. \quad (38)$$

3. Lepton flavor violation

The effective Lagrangian for the lepton flavor violating $l_j\to l_i\gamma$ decay is written as

$$\mathcal{L}_{\rm LFV}=-\frac{e}{16\pi^2}m_{l_j}\bar l_i\frac{i}{2}[\gamma^\mu,\gamma^\nu](A_L^{ij}P_R+A_R^{ij}P_L)l_jF_{\mu\nu},$$
$$(i\neq j), \quad (39)$$

where $P_R=(1+\gamma_5)/2$ and $P_L=(1-\gamma_5)/2$. The decay width is given by

$$\Gamma(l_j\to l_i\gamma)=\frac{\alpha}{64\pi^2}m_{l_j}^5(|A_L^{ij}|^2+|A_R^{ij}|^2). \quad (40)$$

4. Electric dipole moments

Electric dipole moment d_f of a fermion f is defined as the coefficient in the effective Lagrangian

$$\mathcal{L}=\frac{i}{2}d_f\bar f\frac{i}{2}[\gamma^\mu,\gamma^\nu]\gamma_5 fF_{\mu\nu}. \quad (41)$$

In addition, chromoelectric dipole moments of quarks and the three-gluon operator [50] are taken into account for hadronic EDMs. Relevant effective Lagrangian is written as

$$\mathcal{L}=\frac{i}{2}d_q^C\bar q\frac{i}{2}[\gamma^\mu,\gamma^\nu]\gamma_5T^{(a)}qG_{\mu\nu}^{(a)}$$
$$+\frac{d^G}{6}f^{(a)(b)(c)}\epsilon^{\mu\nu\lambda\rho}G_{\mu\sigma}^{(a)}G_\nu^{(b)\sigma}G_{\lambda\rho}^{(a)}. \quad (42)$$

We calculate d_f for quarks and leptons and d_q^C with all the one-loop SUSY contributions [30,31] and two-loop contributions given in Ref. [32]. d^G is calculated according to Ref. [31].

The neutron and the mercury EDMs, $d(n)$ and $d({\rm Hg})$, respectively, are written as linear combinations of d_q, d_q^C, and d^G:

$$d(h)=\sum_{q=u,d,s}[c_q(h)d_q+c_q^C(h)d_q^C]+c^G(h)d^G,$$
$$h=n,{\rm Hg}. \quad (43)$$

Values of the coefficients used in our calculation are given in Table II.

There are large uncertainties in the estimation of the hadronic EDMs. Here we use the value of the neutron EDM obtained by the formulae based on the naive dimensional analysis (NDA) [31]. On the other hand, it has been pointed out that an evaluation with use of the chiral perturbation theory (ChPT) may give a much larger value of the neutron EDM, due to the chromoelectric dipole moment of the strange quark [51]. We later discuss how the numerical results change if the latter is applied.

B. Input parameters and experimental constraints

As input parameters at the low energy, the mass eigenvalues and the flavor mixing matrices of the quarks and leptons are used. We take the top quark mass as $m_t({\rm pole})=170.9$ GeV.

The CKM matrix elements V_{us}, V_{cb}, and $|V_{ub}|$ are determined by measurements of the processes which are supposed to be dominated by the SM tree-level contributions. We adopt $V_{us}=0.224$ and $V_{cb}=0.0416$ in the following calculations. As for the $|V_{ub}|$, because the uncertainty is relatively large, we vary $|V_{ub}|$ within a range $3.0<|V_{ub}|/10^{-3}<4.7$. The CKM phase is not yet determined by tree-level processes free from new physics contributions. Therefore we vary the CKM phase $\phi_3\equiv\arg(-V_{ub}^*V_{ud}/V_{cb}^*V_{cd})$ within $0<\phi_3<180^\circ$.

TABLE II. Hadronic factors used in the calculation of EDMs.

h	c_u	c_d	c_s	c_u^C	c_d^C	c_s^C	c^G	Ref.
n(NDA)	$-\frac{1}{3}$	$\frac{4}{3}$	0	$-\frac{1}{3}\frac{e}{4\pi}$	$\frac{4}{3}\frac{e}{4\pi}$	0	$-\frac{e}{2\sqrt{2}}f_\pi$	[31]
n(ChPT)	0	0	0	$1.6e$	$1.3e$	$0.26e$	0	[51]
Hg	0	0	0	$0.0087e$	$-0.0087e$	$4.4\times10^{-5}e$	0	[51]

In the models with neutrino masses, we need to specify the parameters in the neutrino sector in addition to the quark Yukawa coupling constants. As explained in Sec. II A 2, we consider three cases for the low-energy neutrino mass spectrum and three types for the structure of the neutrino Yukawa coupling matrix. Among nine possible combinations, we show the results of the following five cases:

(i) Degenerate ν_R, normal hierarchy (Dν_R-NH);
(ii) Degenerate ν_R, inverted hierarchy (Dν_R-IH);
(iii) Degenerate ν_R, degenerate (Dν_R-D);
(iv) Nondegenerate ν_R (I), normal hierarchy (NDν_R(I)-NH);
(v) Nondegenerate ν_R (II), normal hierarchy (NDν_R(II)-NH).

In the nondegenerate ν_R cases, we have found that the results do not change much when we take other low-energy neutrino mass spectra, since the neutrino Yukawa coupling matrix is essentially independent of the low-energy neutrino mass spectra. As for the mass eigenvalues, we fix $m^2_{\nu_2} - m^2_{\nu_1} = 8.0 \times 10^{-5}$ eV^2 in all cases. The values of $m^2_{\nu_3} - m^2_{\nu_2}$ and the lightest neutrino mass are shown in Table III. We take the PMNS mixing matrix as

TABLE III. Input parameters for the low-energy neutrino masses. $1-2$ splitting is fixed as $m^2_{\nu_2} - m^2_{\nu_1} = 8.0 \times 10^{-5}$ eV^2 in all cases.

	$m^2_{\nu_3} - m^2_{\nu_2}$ (eV^2)	Lightest ν
Normal hierarchy	2.5×10^{-3}	$m_{\nu_1} = 0.003$ eV
Inverted hierarchy	-2.5×10^{-3}	$m_{\nu_3} = 0.003$ eV
Degenerate	2.5×10^{-3}	$m_{\nu_1} = 0.1$ eV

$$V_{\rm PMNS} = \begin{pmatrix} c_\odot c_{13} & s_\odot c_{13} & s_{13} \\ -s_\odot c_{\rm atm} - c_\odot s_{\rm atm} s_{13} & c_\odot c_{\rm atm} - s_\odot s_{\rm atm} s_{13} & s_{\rm atm} c_{13} \\ s_\odot s_{\rm atm} - c_\odot c_{\rm atm} s_{13} & -c_\odot s_{\rm atm} - s_\odot c_{\rm atm} s_{13} & c_{\rm atm} c_{13} \end{pmatrix}, \tag{44}$$

($c_i = \cos\theta_i$, $s_i = \sin\theta_i$) with $\sin^2 2\theta_{\rm atm} = 1$, $\tan^2\theta_\odot = 0.4$, and $\sin^2 2\theta_{13} = 0$. These mixing angles are consistent with the observed solar and atmospheric neutrino oscillations [2], the K2K experiment [3], and the KamLAND experiment [4]. Only the upper bound of $\sin^2 2\theta_{13}$ is obtained by reactor experiments [5], and we take the above value as an illustration. We ignore the Dirac and Majorana CP phases in the neutrino sector for simplicity, though they can affect the analysis of the lepton flavor violations [52].

The neutrino Yukawa coupling and the right-handed neutrino mass matrices have 18 independent parameters in general. Nine of these parameters are determined by the low-energy neutrino parameters, namely, three masses $m_{\nu_{1,2,3}}$ and $V_{\rm PMNS}$ (three mixing angles and three phases). There remain nine free parameters to specify the neutrino Yukawa coupling and right-handed neutrino mass matrices. In the degenerate ν_R case, these parameters are fixed by the assumption $(M_N)^{ij} = \hat{M}_N \delta^{ij}$, so that y_N is determined as Eq. (12). In the nondegenerate ν_R cases, we take y_N as inputs for the extra nine parameters. We generally parametrize the y_N as

$$y_N = \hat{y}_N V_L, \tag{45}$$

$$\hat{y}_N = {\rm diag}(\hat{y}_1, \hat{y}_2, \hat{y}_3), \tag{46}$$

$$V_L = \begin{pmatrix} \bar{c}_{12}\bar{c}_{13} & \bar{s}_{12}\bar{c}_{13} & \bar{s}_{13} e^{-i\bar{\delta}_{13}} \\ -\bar{s}_{12}\bar{c}_{23} - \bar{c}_{12}\bar{s}_{23}\bar{s}_{13} e^{i\bar{\delta}_{13}} & \bar{c}_{12}\bar{c}_{23} - \bar{s}_{12}\bar{s}_{23}\bar{s}_{13} e^{i\bar{\delta}_{13}} & \bar{s}_{23}\bar{c}_{13} \\ \bar{s}_{12}\bar{s}_{23} - \bar{c}_{12}\bar{c}_{23}\bar{s}_{13} e^{i\bar{\delta}_{13}} & -\bar{c}_{12}\bar{s}_{23} - \bar{s}_{12}\bar{c}_{23}\bar{s}_{13} e^{i\bar{\delta}_{13}} & \bar{c}_{23}\bar{c}_{13} \end{pmatrix} {\rm diag}(e^{i\bar{\psi}_{13}}, e^{i\bar{\psi}_{23}}, 1) e^{-i(\bar{\psi}_{13}+\bar{\psi}_{23})/3}, \tag{47}$$

where $\bar{s}_{ij} = \sin\bar{\theta}_{ij}$ and $\bar{c}_{ij} = \cos\bar{\theta}_{ij}$. The right-handed neutrino mass matrix is written as

$$M_N = \hat{y}_N V_L K_\nu^{-1} V_L^T \hat{y}_N. \tag{48}$$

After calculating M_N, we rescale $\hat{y}_N$ (and M_N) such that M_N satisfies $\det M_N = \mu_R^3$. Therefore, the nine input parameters are $\hat{y}_1/\hat{y}_3$, $\hat{y}_2/\hat{y}_3$, $\bar{s}_{12}$, $\bar{s}_{23}$, $\bar{s}_{13}$, $\bar{\delta}_{13}$, $\bar{\psi}_{13}$, $\bar{\psi}_{23}$, and μ_R. We take the input parameters as shown in Table IV, which provide us with appropriate y_N of the structure (13) and (14). With use of these input parameters, as well as the low-energy neutrino mass spectrum of the normal hierarchy, we obtain the eigenvalues of y_N and M_N at μ_R scale for $\mu_R = 4 \times 10^{14}$ GeV and $\tan\beta = 30$ as $\hat{y}_N = \{0.213, 0.406, 0.647\}$ and $\hat{M}_N = \{2.58, 9.95, 2.49\} \times 10^{14}$ GeV in Case (I) and $\hat{y}_N = \{0.250, 0.469, 0.476\}$ and $\hat{M}_N = \{1.05, 10.2, 5.93\} \times 10^{14}$ GeV in Case (II).

TABLE IV. Input parameters for the neutrino Yukawa coupling matrix in the nondegenerate ν_R cases.

Case	$\hat{y}_1/\hat{y}_3$	$\hat{y}_2/\hat{y}_3$	$\bar{s}_{12}$	$\bar{s}_{23}$	$\bar{s}_{13}$	$\bar{\delta}_{13}$	$\bar{\psi}_{13}$	$\bar{\psi}_{23}$
(I)	0.329	0.628	0	-0.666	0	0	0	0
(II)	0.534	1.014	0	0	0.435	0	0	0

As for the SUSY parameters, we take the convention that the unified gaugino mass $m_{1/2}$ is real. As already described in Sec. II A 1, it is known that ϕ_μ is strongly constrained by the upper bounds of EDMs, while the corresponding constraint on ϕ_A is not so tight [30,31]. Thus we fix $\phi_\mu = 0^\circ$ ($\mu > 0$) at the electroweak scale. We scan the SUSY breaking parameters within the ranges $0 \le m_0 \le 4$ TeV, $0 < m_{1/2} \le 1.5$ TeV ($0 < M_5(\mu_G) \le 1.5$ TeV for SU(5) SUSY GUT with right-handed neutrinos), $|A_0| \le 4$, and $-180^\circ < \phi_A \le 180^\circ$.

In the SU(5) SUSY GUT with right-handed neutrinos, we also vary the two phase parameters, which are introduced at the GUT scale matching as mentioned in Sec. II A 3, within the whole range $\{-180^\circ, 180^\circ\}$.

In the U(2) model, the flavor symmetry breaking parameters ϵ and ϵ' are fixed to be $\epsilon = 0.04$ and $\epsilon' = 0.008$, and the parameters in the quark Yukawa coupling matrices are determined so that the CKM matrix and the quark masses are reproduced. There are six independent $O(1)$ parameters in the quark Yukawa coupling matrices of the form (22) for given quark masses and the CKM matrix. We scan those free parameters as inputs. For the squark mass matrices (23), we make an assumption

$$m_0^{Q2} = m_0^{U2} = m_0^{D2} = m_0^2, \tag{49}$$

and scan the range of m_0 as $0 < m_0 < 4$ TeV. Dimensionless parameters in Eq. (23) are varied within the ranges $0.4 \le r_{22}^X$, r_{33}^X, $|r_{23}^X| \le 2.5$, and $-180^\circ < \arg r_{23}^X \le 180^\circ$. We assume that the boundary conditions for the A parameters are the same as the mSUGRA case for simplicity.[1]

In order to constrain the parameter space, we consider the following experimental results:

(i) Lower limits on the masses of SUSY particles and the Higgs bosons given by direct searches in collider experiments [53].

(ii) Branching ratio of the $b \to s\gamma$ decay: $\mathrm{B}(b \to s\gamma) = (3.55 \pm 0.24^{+0.09}_{-0.10} \pm 0.03) \times 10^{-4}$ [54]. We take the allowed range for the calculated branching ratio as $2.85 \times 10^{-4} < \mathrm{B}(b \to s\gamma) < 4.25 \times 10^{-4}$, also taking account of theoretical uncertainties.

(iii) Upper bounds of the branching ratios of the $\mu \to e\gamma$, $\tau \to \mu\gamma$, and $\tau \to e\gamma$ decays for the MSSM with right-handed neutrinos and SUSY GUT cases: $\mathrm{B}(\mu \to e\gamma) < 1.2 \times 10^{-11}$ [55], $\mathrm{B}(\tau \to \mu\gamma) < 6.8 \times 10^{-8}$ [56], and $\mathrm{B}(\tau \to e\gamma) < 1.1 \times 10^{-7}$ [57]. Upper bounds of EDMs of ^{199}Hg, the neutron and the electron: $|d_{\mathrm{Hg}}| < 2.1 \times 10^{-28} e \cdot \mathrm{cm}$ [58], $|d_n| < 2.9 \times 10^{-26} e \cdot \mathrm{cm}$ [59], and $|d_e| < 1.6 \times 10^{-27} e \cdot \mathrm{cm}$ [60].

(iv) The CP violation parameter ε_K in the $K^0 - \bar{K}^0$ mixing $|\varepsilon_K| = (2.232 \pm 0.007) \times 10^{-3}$ and the $B_d - \bar{B}_d$ and the $B_s - \bar{B}_s$ mixing parameters $\Delta m_{B_d} = 0.507 \pm 0.005\ \mathrm{ps}^{-1}$ [61] and $\Delta m_{B_s} = 17.77 \pm 0.10 \pm 0.07\ \mathrm{ps}^{-1}$ [62]. Theoretical uncertainties in these quantities are larger than the experimental ones. For the $B - \bar{B}$ mixings, 1σ uncertainties of the decay constants $f_{B_{d,s}}$ and of the bag parameters $B_{B_{d,s}}$ are evaluated as 10% and 8%, respectively [44]. In the present analysis, we calculate $\Delta m_{B_{d,s}}$ with a fixed set of hadronic parameters as listed in Table I and allow ± 40 percent deviations from the experimental central values. We expect that these ranges provide typical $2 - 3\sigma$ allowed intervals. In addition, the ratio of the hadronic parameters $\xi \equiv f_{B_s}\sqrt{B_{B_s}}/(f_{B_d}\sqrt{B_{B_d}})$ is evaluated with better accuracy. The uncertainty of ξ is evaluated as ± 4 percent [44]. Therefore we also require that the calculated ratio $\Delta m_{B_s}/\Delta m_{B_d}$, which is proportional to ξ^2, be within ± 20 percent range of the central value. For ε_K we assign ± 15 percent uncertainty.

(v) CP asymmetry in the $B_d \to J/\psi K_S$ decay and related modes observed at the B factory experiments: $\sin 2\phi_1|_{c\bar{c}s} = 0.678 \pm 0.025$ [61]. We take the allowed range for the calculated value as $0.628 < S_{CP}(B_d \to J/\psi K_S) < 0.728$, which is a simple 2σ interval, since the theoretical uncertainty of this asymmetry is expected to be small.

C. Numerical results

1. Allowed parameter region from the radiative electroweak symmetry breaking condition

Before presenting flavor signals, we first discuss the SUSY parameter space which is allowed by the radiative electroweak symmetry breaking condition and experimental constraints.

In Fig. 2, we show the allowed region in the m_0 and $m_{1/2}$ plane for the mSUGRA, MSSM with right-handed neutrinos, and SU(5) SUSY GUT with right-handed neutrinos. Parameters other than m_0 and $m_{1/2}$ are fixed as indicated in each plot. Contours of $|\mu|$ determined from the electroweak symmetry breaking condition are also shown. In mSUGRA, the parameter region is mainly constrained by the lower limit on the chargino mass, the limit on the lightest Higgs boson mass, the branching ratio of $b \to s\gamma$ decay, and the requirement that the lightest supersymmetric particle (LSP) is neutral. When the neutrino Yukawa couplings are relevant, the lepton flavor violating decays are enhanced. As a result, a large portion is excluded due to the experimental upper limit on the branching ratio of $\mu \to e\gamma$ for MSSM with right-handed neutrinos and SU(5) SUSY GUT with right-handed neutrinos. Notice that we

[1] We have carried out a preliminary analysis of the flavor signals for the case with nonuniversal A terms, where A_Q^0, $\tilde{a}_Q$, $\tilde{b}_Q$, $\tilde{c}_Q$, and $\tilde{d}_Q$ in Eq. (24) are free $O(1)$ parameters with a small number of samples. We have found that the EDMs become too large in most of the parameter sets chosen at random. The result of the flavor signals does not change much once the EDM constraints are applied.

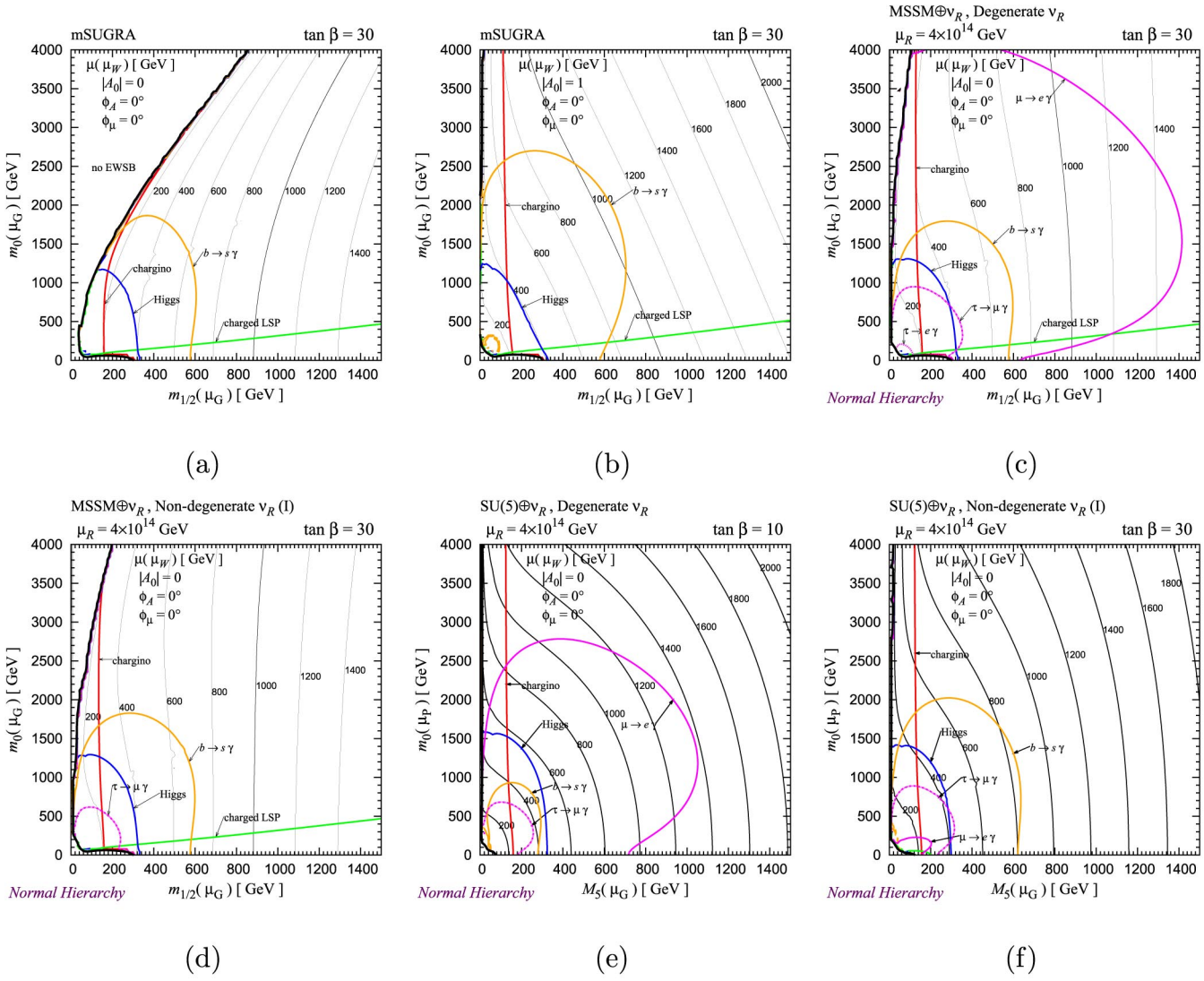

FIG. 2 (color online). Contour plots of the value of $|\mu|$ on m_0 and $m_{1/2}$ plane for fixed $\tan\beta$ and A_0 in mSUGRA ((a) and (b)), MSSM with right-handed neutrinos ((c) and (d)), and SU(5) SUSY GUT with right-handed neutrinos models ((e) and (f)). Each thick black line shows the boundary of the region where correct electroweak symmetry breaking occurs. In the regions below the lines labeled with "charged LSP" (green) in (a)–(d), the LSP is a charged particle. Boundaries of excluded regions which come from the chargino mass ("chargino"/red), the Higgs boson mass ("Higgs"/blue) and B($b \to s\gamma$) ("$b \to s\gamma$"/orange) are shown in each plot. Regions excluded by the lepton flavor violating processes are also shown in (c)–(f) ("$\mu \to e\gamma$," "$\tau \to \mu\gamma$" or "$\tau \to e\gamma$"/magenta).

take *CP* violating SUSY phases to be vanishing in these plots. A significant potion of the parameter space is excluded due to the experimental limits on EDMs if we take nonvanishing SUSY *CP* phases.

In the plot for mSUGRA with $|A_0| = 0$ (Fig. 2(a)), the $m_0 \gg m_{1/2}$ region is excluded because the electroweak symmetry breaking cannot be satisfied, namely, there is no solution with $|\mu|^2 \geq 0$ for this region. The allowed region near the boundary corresponds to the so-called "focus point" region [63] where the LSP is the lightest neutralino with a significant higgsino component. This region is one of the favored regions in the context of the cosmic dark matter study [64]. The pair annihilation of the lightest neutralino into the W boson or Z boson pair is enhanced by the gauge interaction of the higgsino component, so that the relic abundance of the LSP becomes suitable for the cold dark matter density. However, in the $|A_0| = 1$ case (Fig. 2(b)), such a region disappears because the A-terms affect the running of the Higgs mass parameter $m_{H_2}^2$ so that a sufficiently large $|\mu|^2$ is realized. The "focus point"–like region disappears also in the cases with right-handed neutrinos (Figs. 2(c)–2(f)), since the large neutrino Yukawa coupling affects the running of $m_{H_2}^2$ in a similar way.

In the cases of mSUGRA and MSSM with right-handed neutrinos (Figs. 2(a)–2(d)), the $m_0 \ll m_{1/2}$ region is excluded because the LSP is the lightest charged slepton. The allowed region near the boundary provides another dark

matter favored region [65]. The coannihilation effect among the LSP (neutralino) and the next-to-LSP (slepton), which are nearly degenerate in mass, provides an appropriate relic abundance of LSP. On the other hand, in the SU(5) SUSY GUT with right-handed neutrinos (Figs. 2(e) and 2(f)), the running between the Planck and the GUT scales induces positive contribution to the slepton mass squared, which makes the charged slepton heavier than the lightest neutralino even in the $m_0 \ll m_{1/2}$ region. Therefore the "charged LSP" or "stau coannihilation" region disappears in the SU(5) SUSY GUT with right-handed neutrinos.

The disappearance of the "focus point"–like region due to the effect of the neutrino Yukawa couplings and the disappearance of the "charged LSP" region caused by the running between the Planck and the GUT scales are previously observed in Ref. [26], where the SO(10) SUSY GUT is considered.

2. Lepton flavor violating μ and τ decays

There are lepton flavor mixings in the slepton sector of the MSSM with right-handed neutrinos and the SU(5) SUSY GUT with right-handed neutrinos. It comes through the running between the right-handed neutrino mass scale and the cutoff scale where the universal soft breaking mass terms are generated. On the other hand, no such slepton flavor mixings exist in the mSUGRA.

In Figs. 3 and 4, the branching ratios of $\mu \to e\gamma$, $\tau \to \mu\gamma$, and $\tau \to e\gamma$ are displayed as a function of the lightest charged slepton mass $m(\tilde{l}_1)$ for the MSSM with right-handed neutrinos and the SU(5) SUSY GUT with right-handed neutrinos, respectively. For each model, we show the results for five cases of the neutrino masses and Yukawa coupling matrix as explained in Sec. III B. The right-handed neutrino mass scale μ_R is taken as $\mu_R = 4 \times 10^{14}$ GeV for the normal and inverted hierarchy cases,

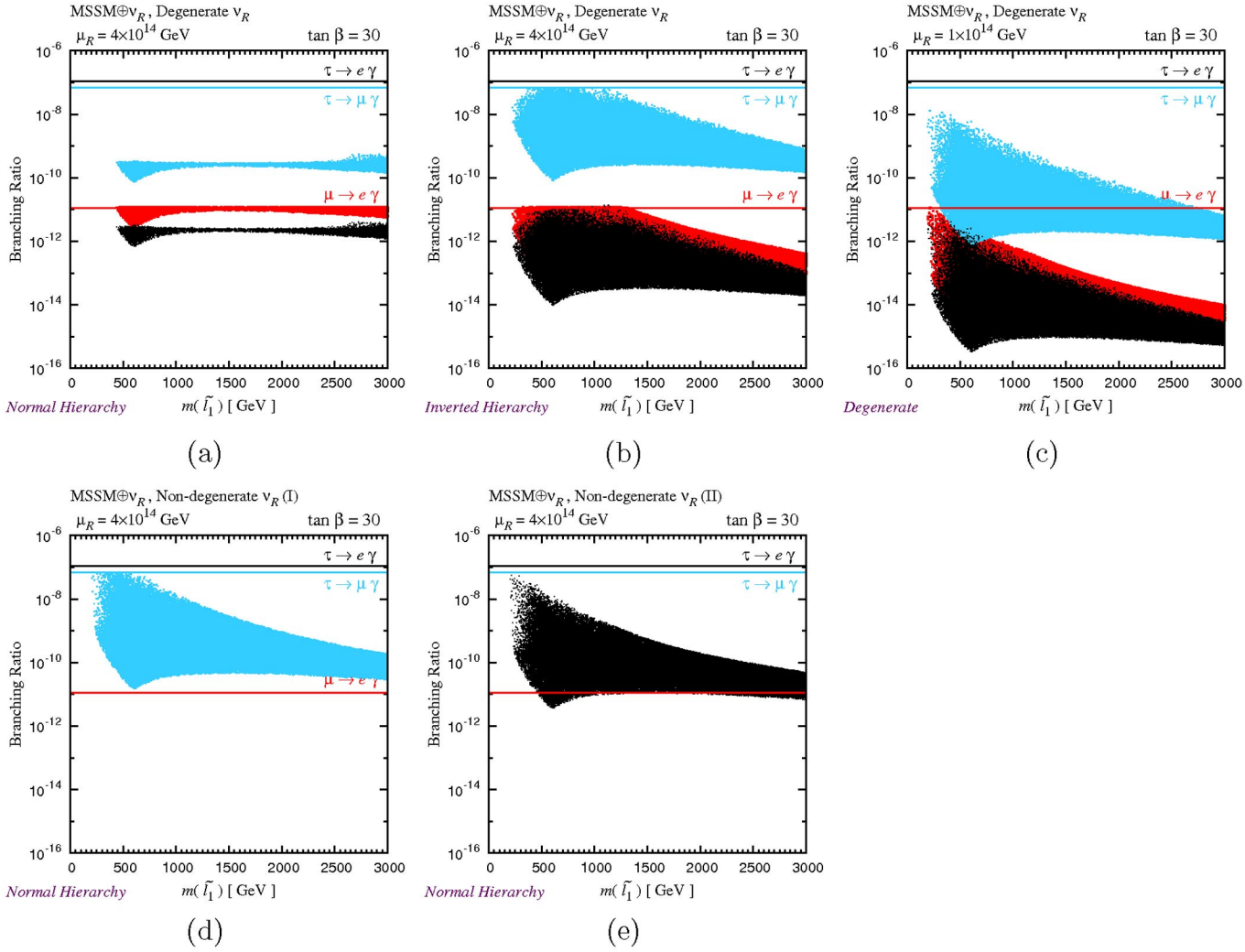

FIG. 3 (color online). Branching ratios of lepton flavor violation processes $\mu \to e\gamma$ (gray/red), $\tau \to \mu\gamma$ (light-gray/light-blue), and $\tau \to e\gamma$ (black) as functions of the lightest charged slepton mass $m(\tilde{l}_1)$ for MSSM with right-handed neutrinos. Horizontal lines denote experimental upper limits. In the plot (d), $\mu \to e\gamma$ and $\tau \to e\gamma$ are strongly suppressed. In the plot (e), $\mu \to e\gamma$ and $\tau \to \mu\gamma$ are strongly suppressed.

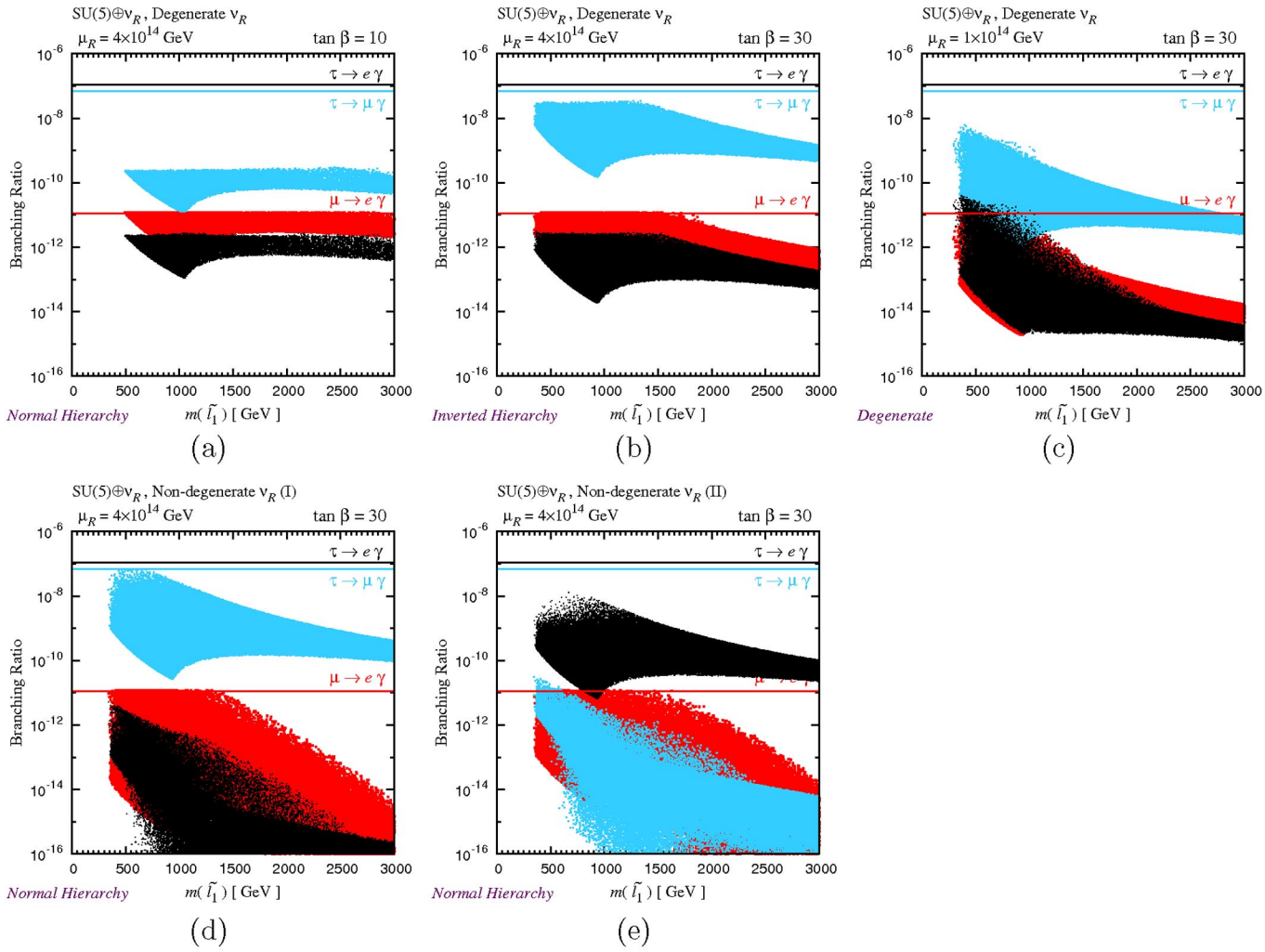

FIG. 4 (color online). Branching ratios of lepton flavor violation processes as functions of the lightest charged slepton mass for SU(5) SUSY GUT with right-handed neutrinos. Notations are the same as those in Fig. 3.

which corresponds to the neutrino Yukawa couplings of $O(1)$. In the degenerate ($m_{\nu_1} = 0.1$ eV) case, we take $\mu_R = 1 \times 10^{14}$ GeV since the neutrino Yukawa coupling blows up below the Planck scale for $\mu_R = 4 \times 10^{14}$ GeV. It is known that branching ratios are enhanced by a factor of $\tan^2\beta$ for large values of $\tan\beta$. In the presented plots, we take $\tan\beta = 30$ except for the case of the degenerate ν_R with normal hierarchical neutrinos (Dν_R-NH) in the SU(5) SUSY GUT with right-handed neutrinos, where we show the result for $\tan\beta = 10$. When we take $\tan\beta = 30$ for Dν_R-NH in the SU(5) SUSY GUT with right-handed neutrinos, almost all the data points in the scanned parameter space are excluded due to the B($\mu \to e\gamma$) constraint.

We can see that the $\mu \to e\gamma$ decay rate is enhanced in the normal hierarchy with degenerate ν_R cases. In fact, even for the slepton as heavy as 3 TeV, B($\mu \to e\gamma$) is close to (or above) the experimental upper limit. After applying the constraint from B($\mu \to e\gamma$), the branching ratio of $\tau \to \mu\gamma$ can be 10^{-9} at most. On the other hand, in the inverted hierarchy and degenerate cases (with degenerate ν_R), $\mu \to e\gamma$ and $\tau \to e\gamma$ are relatively suppressed. This behavior is understood in the following way. From the neutrino Yukawa coupling matrix (12) and the PMNS matrix (44) with $s_{13} = 0$, the off-diagonal elements of $y_N^\dagger y_N$ are written as

$$(y_N^\dagger y_N)_{12} = \frac{\hat{M}_N}{\langle h_2\rangle^2} c_\odot s_\odot c_{\rm atm} \frac{m_{\nu_2}^2 - m_{\nu_1}^2}{m_{\nu_2} + m_{\nu_1}},$$
$$(y_N^\dagger y_N)_{13} = -\frac{\hat{M}_N}{\langle h_2\rangle^2} c_\odot s_\odot s_{\rm atm} \frac{m_{\nu_2}^2 - m_{\nu_1}^2}{m_{\nu_2} + m_{\nu_1}}. \quad (50)$$

Therefore the $1-2$ and $1-3$ slepton mixings are suppressed for a larger value of $m_{\nu_2} + m_{\nu_1}$ when $m_{\nu_2}^2 - m_{\nu_1}^2$ and $\hat{M}_N = \mu_R$ are fixed.

In the nondegenerate ν_R (I) case, B($\mu \to e\gamma$) is suppressed compared to the degenerate ν_R cases, so that the constraint is weakened. In particular, there is an approximate electron-number conservation in the MSSM with right-handed neutrinos with the Yukawa coupling matrix

of the structure Eq. (13), which leads to the suppression of both $\mu \to e\gamma$ and $\tau \to e\gamma$. The branching ratio of $\tau \to \mu\gamma$ can be as large as the current experimental upper limit. In the SU(5) SUSY GUT with right-handed neutrinos, the electron-number conservation is broken by GUT interactions. As a result, $B(\mu \to e\gamma)$ can be also as large as the current experimental upper limit. In the nondegenerate ν_R (II) cases, the role of e and μ are interchanged due to the Yukawa structure Eq. (14).

Correlations between $B(\tau \to \mu(e)\gamma)$ and $B(\mu \to e\gamma)$ in the SU(5) SUSY GUT with right-handed neutrinos are shown in Fig. 5. Since the MEG experiment can measure $B(\mu \to e\gamma)$ down to 10^{-13} and the Super B factory can measure $B(\tau \to \mu\gamma)$ and $B(\tau \to e\gamma)$ of 10^{-9}, it is possible to distinguish the structure of the slepton flavor mixing if the slepton mass is less than 1 TeV.

3. Quark flavor signals

We show quark flavor signals in the mSUGRA, SU(5) SUSY GUT with right-handed neutrinos and the U(2) flavor symmetry models. In the MSSM with right-handed neutrinos, there is no new source of the squark flavor mixing other than the CKM matrix. The effect of the neutrino Yukawa couplings appears in the squark sector only through the renormalization of the Higgs fields. Consequently the flavor structure of the squarks is essentially the same as the mSUGRA case. In fact, we have checked that the plots of the quark flavor signals look similar to those in the mSUGRA, except that the allowed SUSY parameter region is largely affected by the constraints from the LFV processes. That is why we do not show the plots in the MSSM with right-handed neutrinos here. Quark flavor signals in the SU(5) SUSY GUT with

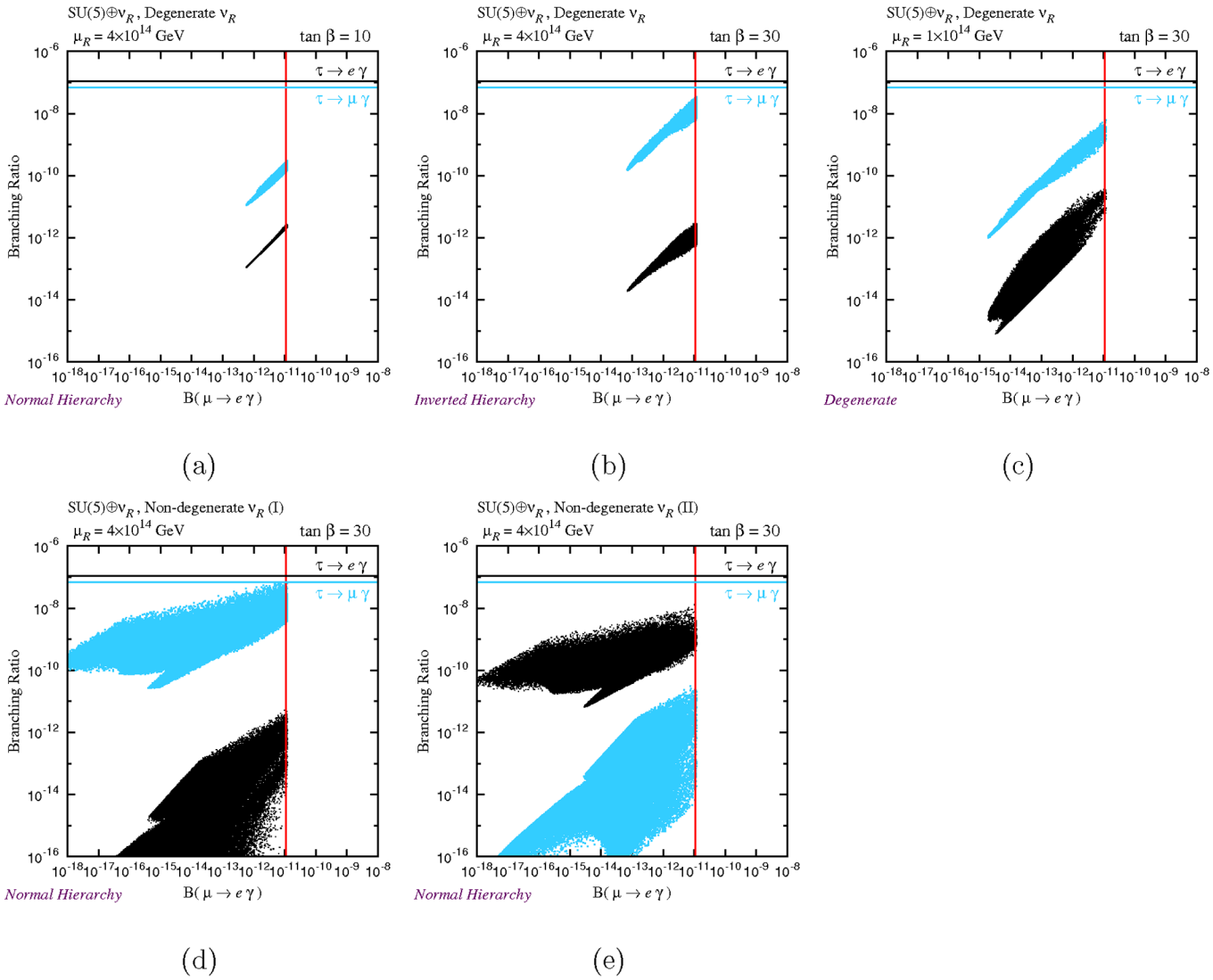

FIG. 5 (color online). Correlations between $B(\tau \to \mu(e)\gamma)$ and $B(\mu \to e\gamma)$. Light-gray (light-blue) and black dots denote $\tau \to \mu\gamma$ and $\tau \to e\gamma$, respectively. Experimental upper limits of the branching ratios are shown by horizontal and vertical lines in each plot.

right-handed neutrinos are affected by the existence of the neutrino Yukawa coupling through the GUT running between μ_P and μ_G. Large $b-s$ and $b-d$ mixings in the right-handed down-type squark sector are induced by the large $2-3$ and $1-3$ mixing in the neutrino Yukawa coupling in the nondegenerate ν_R (I) and (II) cases, respectively. In the degenerate ν_R cases, the parameter region excluded by the $\mu \to e\gamma$ constraint depends on the low-energy neutrino mass spectrum. In particular, the region with sizable squark mixings is excluded due to the strong $\mu \to e\gamma$ constraint in the normal hierarchy case. On the other hand, the region with large $2-3$ squark mixing remains in the inverted hierarchy case. The U(2) model has large $2-3$ mixings in both the right-handed and left-handed squark sector at the cutoff scale.

Here we show our results on the following observables:

(i) The direct CP asymmetry in $b \to s\gamma$ decay (Fig. 6), which is sensitive to the effect of the new CP violating phase in the $b \to s\gamma$ decay amplitude.

(ii) The mixing-induced CP asymmetry in $B_d \to K^*\gamma$ (Fig. 7). This asymmetry is enhanced by the $b \to s\gamma$ decay amplitude with the chirality opposite to the SM one.

(iii) The direct CP asymmetry in $b \to d\gamma$ decay (Fig. 8), which is sensitive to the effect of the new CP violating phase in the $b \to d\gamma$ decay amplitude.

(iv) The mixing-induced CP asymmetry in $B_d \to \rho\gamma$ (Fig. 9), which is enhanced by the $b \to d\gamma$ decay amplitude with the chirality opposite to the SM one.

(v) The mixing-induced CP asymmetry in $B_d \to \phi K_S$ decay (Fig. 10). The difference between this quantity and the mixing-induced CP asymmetry in $B_d \to J/\psi K_S$, $\Delta S_{CP}(B_d \to \phi K_S) \equiv S_{CP}(B_d \to \phi K_S) - S_{CP}(B_d \to J/\psi K_S)$ is sensitive to the new CP violating phase in the $b \to s\bar{s}s$ decay amplitude.

(vi) The mixing-induced CP asymmetry in $B_s \to J/\psi\phi$ decay (Fig. 11), which is affected by the new CP violating phase in the $B_s - \bar{B}_s$ mixing matrix element.

From Figs. 6–11, we can draw the following conclusions. For the mSUGRA case, we do not see significant deviations in any of the above observables. In the cases of the degenerate ν_R with normal hierarchical (light) neutrinos (Dν_R-NH) and the degenerate ν_R with degenerate neutrinos (Dν_R-D) for the SU(5) SUSY GUT with right-handed neutrinos, the parameter region is strongly constrained by the B($\mu \to e\gamma$) as already discussed. There are some points in which deviations are apparent in $S_{CP}(B_d \to K^*\gamma)$, $S_{CP}(B_d \to \rho\gamma)$, $\Delta S_{CP}(B_d \to \phi K_S)$, and $S_{CP}(B_s \to J/\psi\phi)$. These points could be distinguished by future measurements such as LHCb, in which the precision in the determination of the phase of the $B_s - \bar{B}_s$ mixing

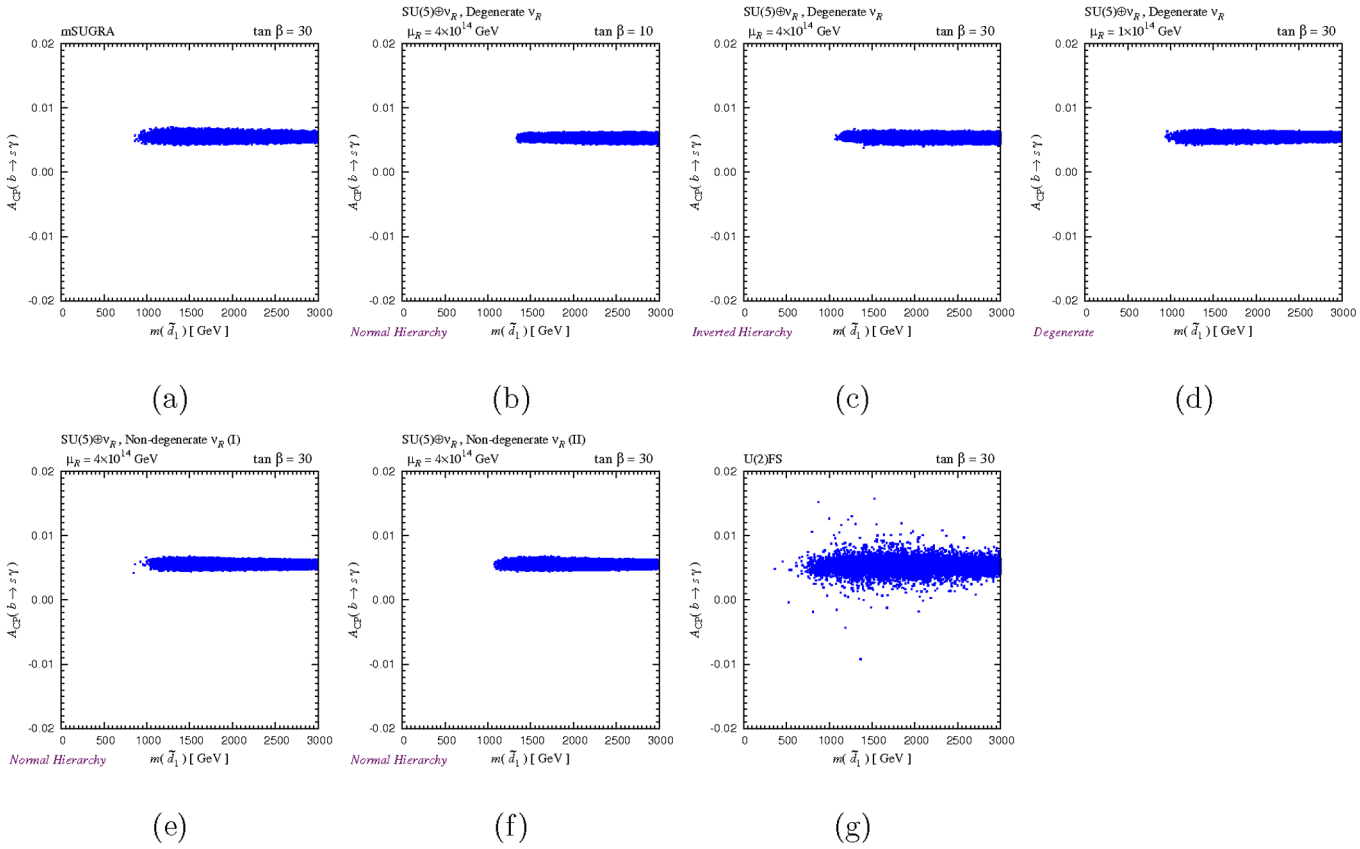

FIG. 6 (color online). The direct CP asymmetry in $b \to s\gamma$ as functions of the lightest down-type squark mass $m(\tilde{d}_1)$ for (a) mSUGRA, (b)–(f) five cases of the SU(5) SUSY GUT with right-handed neutrinos, and (g) U(2) model.

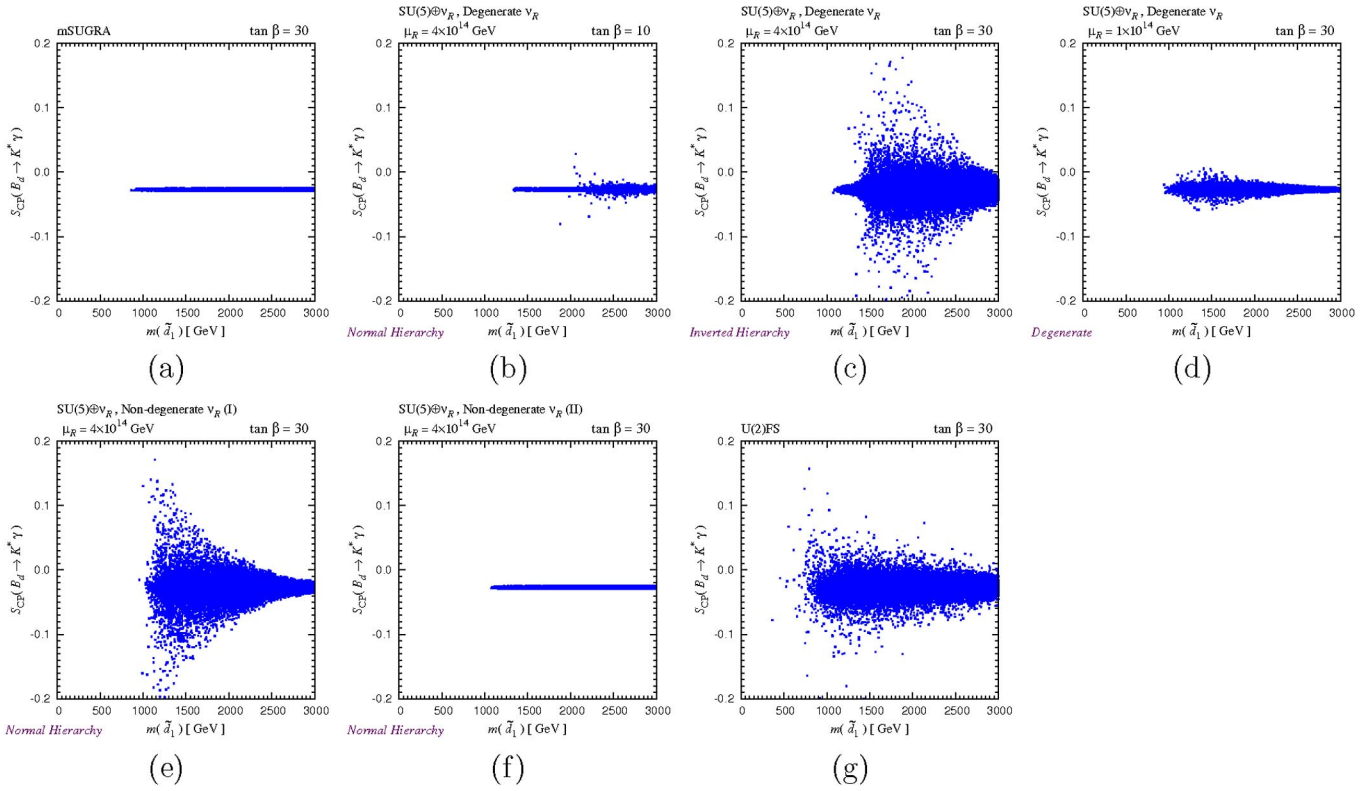

FIG. 7 (color online). The mixing-induced CP asymmetry in $B_d \to K^*\gamma$ as functions of $m(\tilde{d}_1)$ for the same parameter sets as those for Fig. 6.

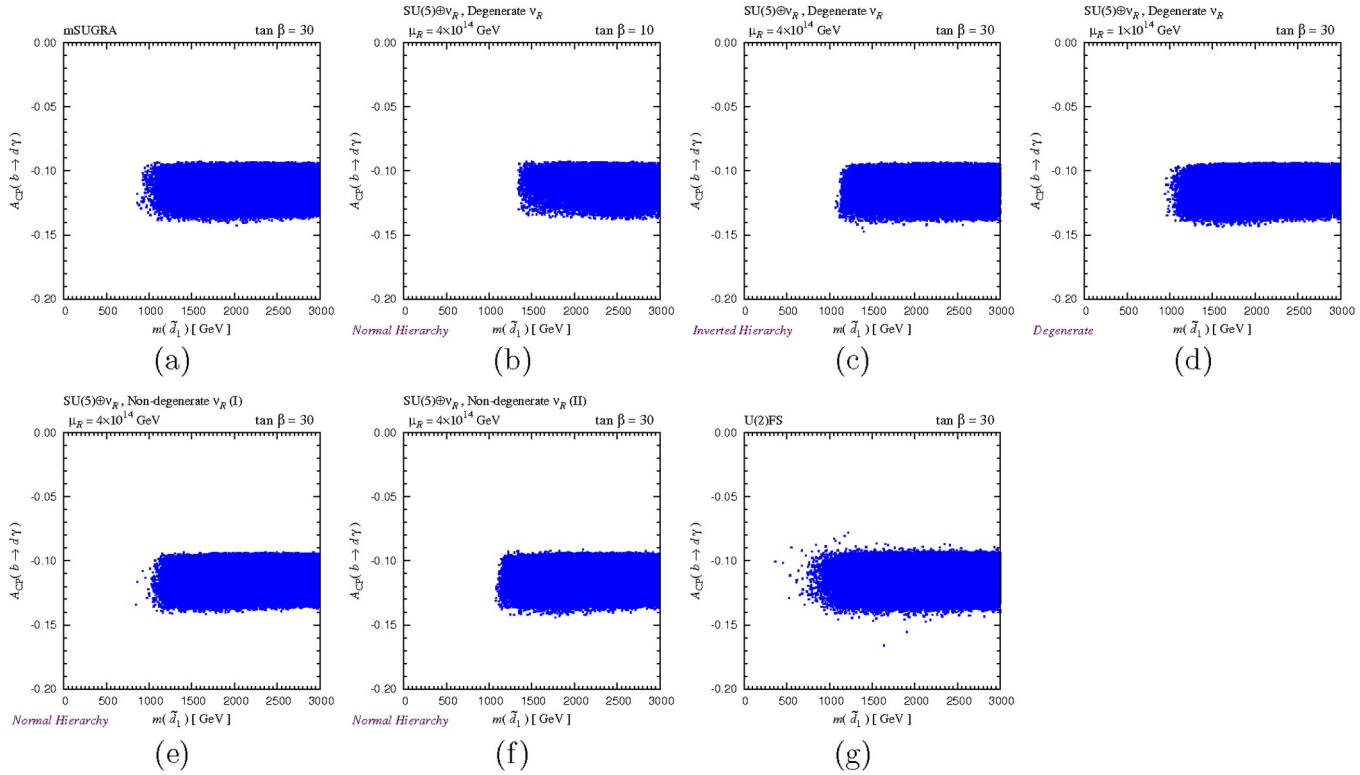

FIG. 8 (color online). The direct CP asymmetry in $b \to d\gamma$ as functions of $m(\tilde{d}_1)$ for the same parameter sets as those for Fig. 6.

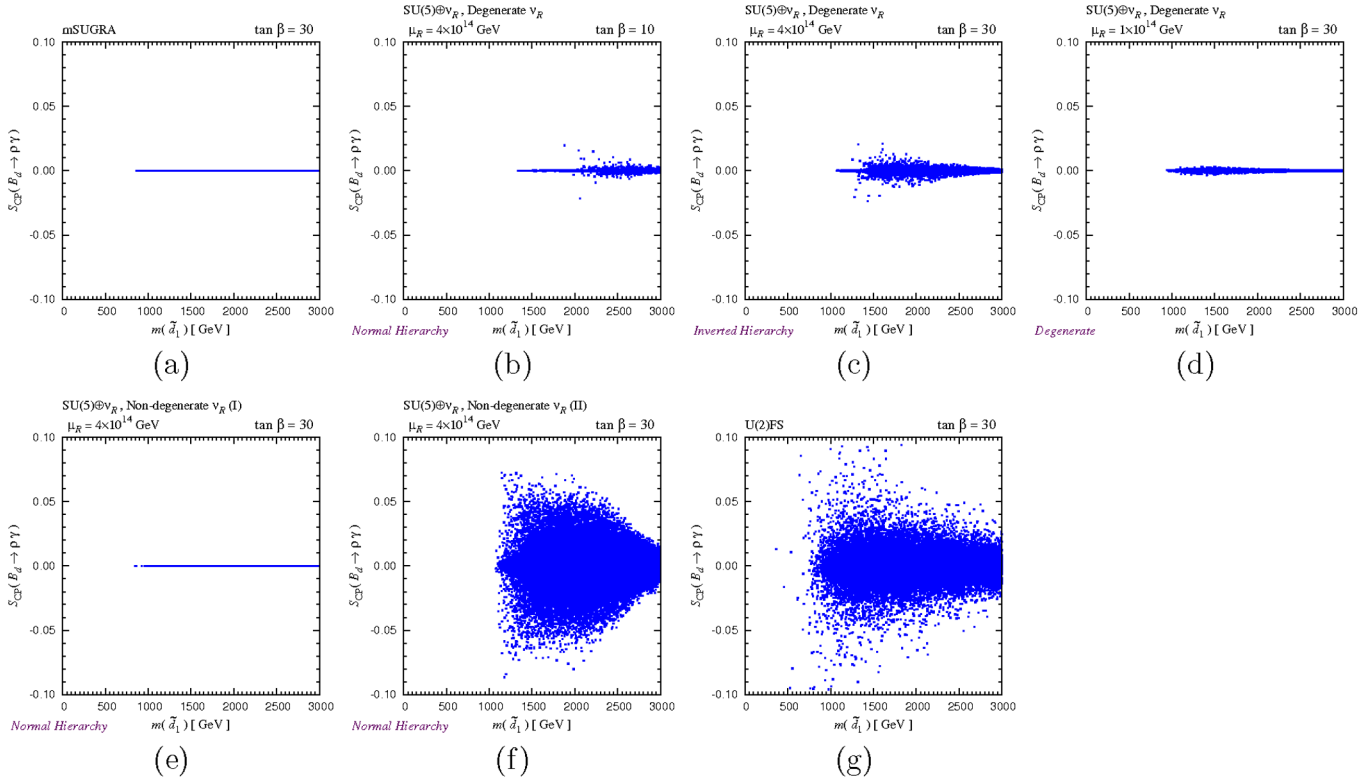

FIG. 9 (color online). The mixing-induced CP asymmetry in $B_d \to \rho\gamma$ as functions of $m(\tilde{d}_1)$ for the same parameter sets as those for Fig. 6.

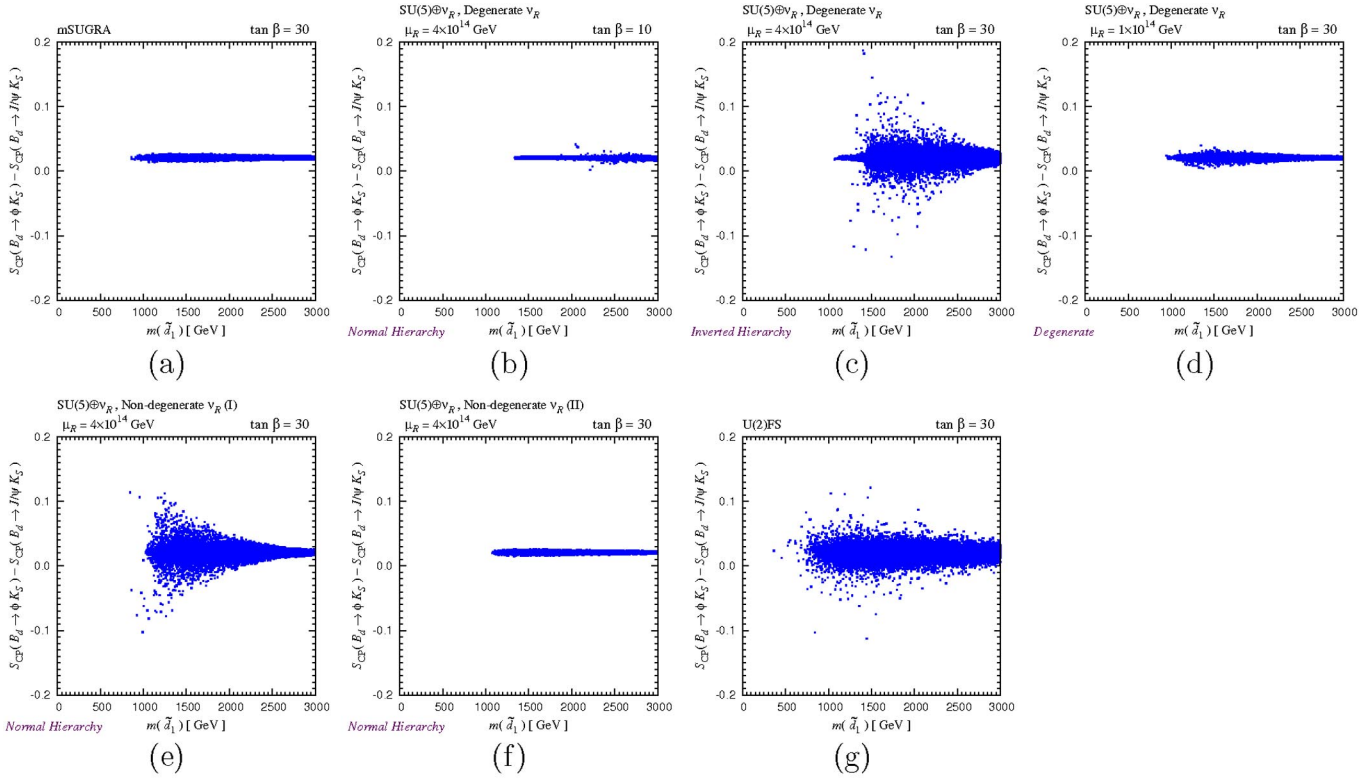

FIG. 10 (color online). The difference between mixing-induced CP asymmetries in the $B_d \to \phi K_S$ and $B_d \to J/\psi K_S$ modes as functions of $m(\tilde{d}_1)$ for the same parameter sets as those in Fig. 6.

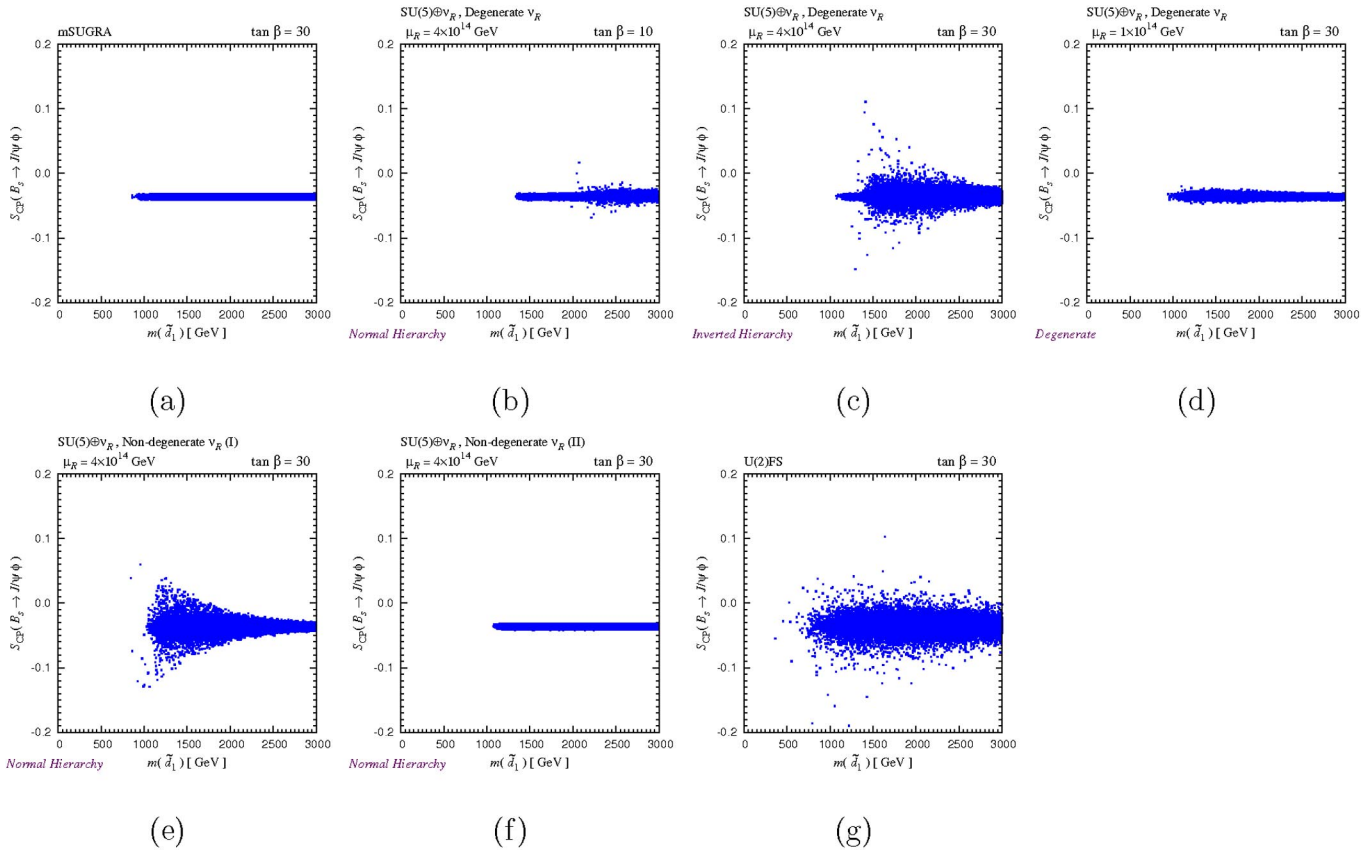

FIG. 11 (color online). Predicted value of the mixing-induced CP asymmetry in $B_s \to J/\psi\phi$ as a function of $m(\tilde{d}_1)$ for the same parameter sets as those for Fig. 6.

matrix element is expected to be 0.01 rad level [12]. In the degenerate ν_R with inverted hierarchical neutrinos (Dν_R-IH) and the nondegenerate ν_R (I) with normal hierarchical neutrinos (NDν_R(I)-NH) cases of the SU(5) SUSY GUT with right-handed neutrinos, the SUSY contributions to mixing-induced CP asymmetries in $B_s \to J/\psi\phi$, $B_d \to K^*\gamma$, and $B_d \to \phi K_S$ can be significant. On the other hand, in the nondegenerate ν_R (II) with normal hierarchical neutrinos (NDν_R(II)-NH) case of SU(5) SUSY GUT with right-handed neutrinos, there is a significant SUSY contribution to the $b \to d\gamma$ decay amplitude, so that $S_{CP}(B_d \to \rho\gamma)$ can be as large as ± 0.1. Large SUSY contributions can be found for almost all modes we analyze in the U(2) model. Only the direct CP asymmetry in $b \to d\gamma$ does not show any significant deviation from the SM.

The correlation between ϕ_3 and $\Delta m_{B_s}/\Delta m_{B_d}$ is shown in Fig. 12. $\Delta m_{B_s}/\Delta m_{B_d}$ is sensitive to the new physics contributions to the $B_d - \bar{B}_d$ and $B_s - \bar{B}_s$ mixing matrix elements unless the contributions cancel in the ratio. For the mSUGRA case, the deviation is negligible and the plot in this plane is the same as in the SM. The lower limit of ϕ_3 is determined by the constraint from ε_K. In the Dν_R-NH and Dν_R-D cases of SU(5) SUSY GUT with right-handed neutrinos, the deviation in the correlation is not so significant. In the Dν_R-IH and the nondegenerate ν_R cases of SU(5) SUSY GUT with right-handed neutrinos, as well as the U(2) model, some deviations appear in the correlation plots. In the Dν_R-IH and NDν_R(I)-NH cases the deviation comes from the SUSY contribution to the $B_s - \bar{B}_s$ mixing matrix element, while $B_d - \bar{B}_d$ receive sizable SUSY correction in NDν_R(II)-NH. In the U(2) model SUSY contributions show up in both matrix elements. In order to identify the deviation in the correlation in the future, it is required that the evaluation of the ξ parameter by the lattice QCD calculation is significantly improved and that the ϕ_3 is precisely measured from tree-level dominant processes.

In Fig. 13, we show the correlations among $S_{CP}(B_d \to K^*\gamma)$, $\Delta S_{CP}(B_d \to \phi K_S)$, $S_{CP}(B_s \to J/\psi\phi)$, and $\mathrm{B}(\tau \to \mu\gamma)$ for Dν_R-IH and NDν_R(I)-NH cases of the SU(5) SUSY GUT with right-handed neutrinos, where these quantities are significantly affected. We can see that large deviations in $b \to s$ transitions occur in the region with $\mathrm{B}(\tau \to \mu\gamma) \gtrsim 10^{-9}$. Also there is a positive correlation between $S_{CP}(B_d \to K^*\gamma)$ and $\Delta S_{CP}(B_d \to \phi K_S)$.

We also calculate the branching ratio and the forward-backward asymmetry of $b \to s l^+ l^-$, which are sensitive to the amplitudes from photon- and Z-penguin and box diagrams. In all the cases we consider here, we find the deviations are negligible.

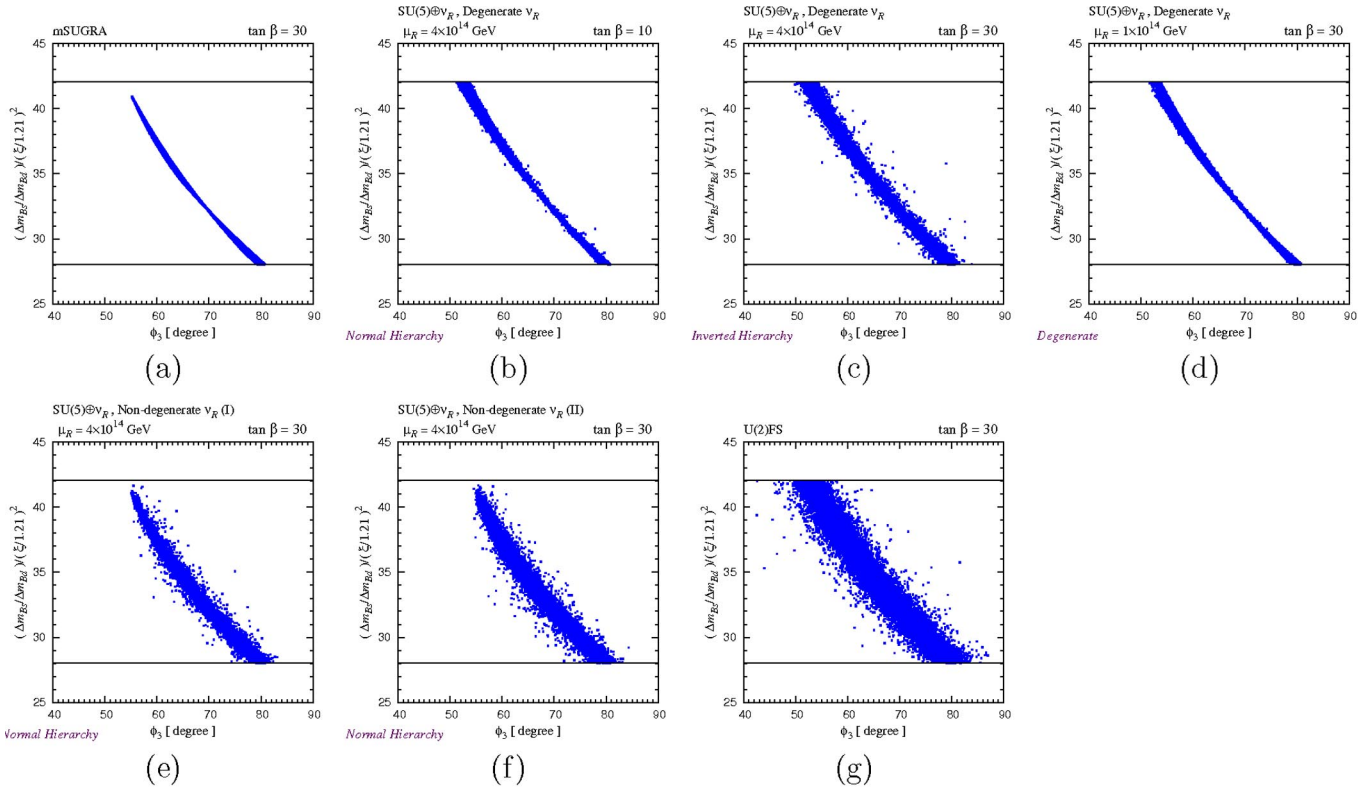

FIG. 12 (color online). Correlation between ϕ_3 and $\Delta m_{B_s}/\Delta m_{B_d}$ for the same parameter sets as those in Fig. 6.

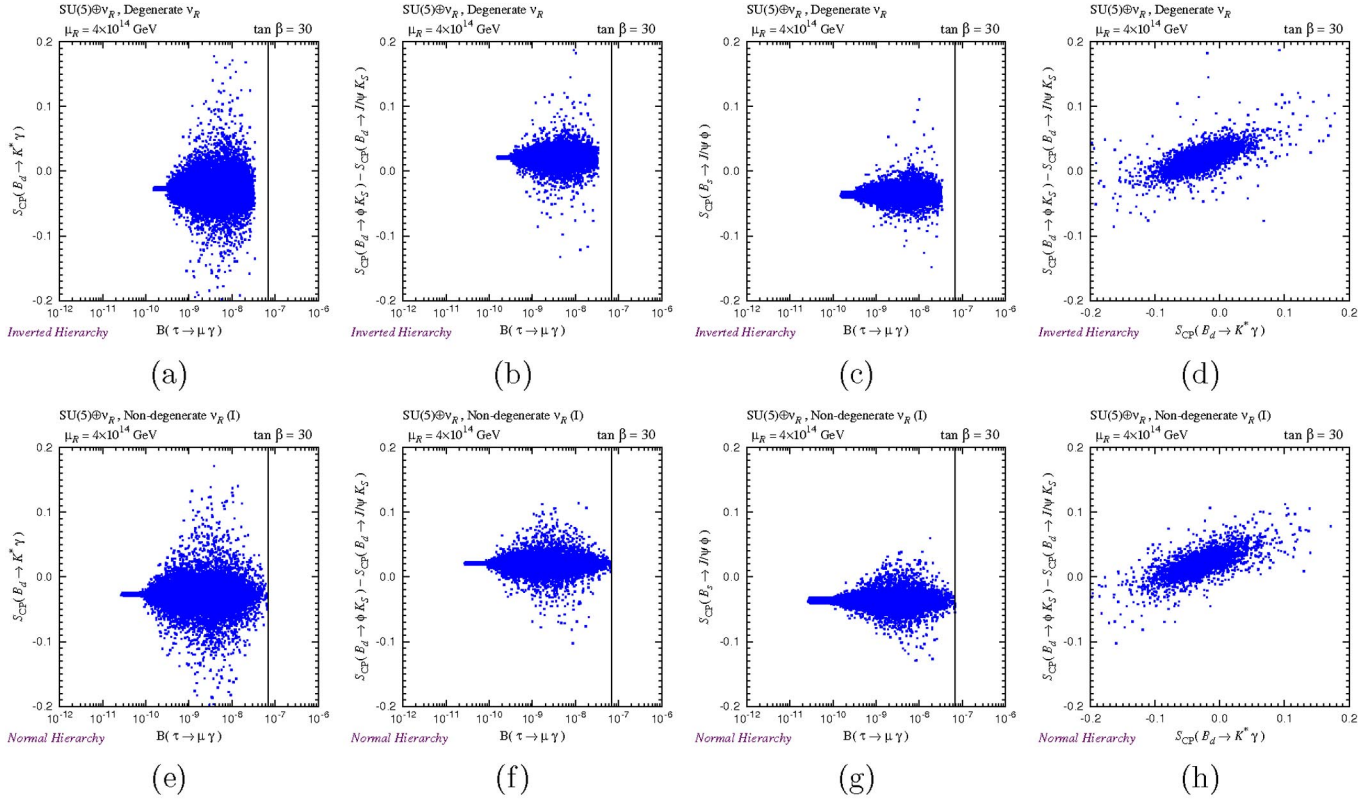

FIG. 13 (color online). Correlations among $b \to s$ observables and $\mathrm{B}(\tau \to \mu\gamma)$.

4. EDM constraints

We show the EDMs of the neutron, ^{199}Hg and the electron as functions of the lightest down-type squark mass in Fig. 14. Here we use the NDA formula for the neutron EDM. The primary source of these EDMs is the phase of the A_0, since we fix the phase of the higgsino mass parameter as $\phi_\mu = 0$ in the present analysis. The EDMs for $\phi_\mu = O(1)$ are larger than those for $\phi_\mu = 0$ by 1 or 2 orders of magnitude and easily exceed the experimental upper limits in large portions of the parameter space. In the present case, we can see that the upper limit of the electron EDM mainly constrains the parameter space, while the constraints from other two EDMs are slightly weaker.

Let us discuss how the possible quark and lepton flavor signals change if we use the formula for the neutron EDM based on the chiral perturbation theory, as mentioned in Sec. III A 4. The main difference between the NDA and ChPT formulae is the treatment of the strange quark (chromo-)EDM. In ChPT the contribution from the strange quark is taken into account, while it is simply neglected in NDA. In the NDν_R(I)-NH and Dν_R-IH of the SU(5) SUSY GUT with right-handed neutrinos and the U(2) cases, the two- to three-generation mixings and CP violating phases exist in both left- and right-handed down-type squark mass matrices, which enhance the chromo-EDM of the strange quark. Therefore, the SUSY contributions to the CP asymmetries in $b \to s$ decays correlate to the chromo-EDM of the strange quark.

We show the plots of the neutron EDM calculated by the ChPT formula [51] in Fig. 15. It can be seen that the ChPT formula leads to typically $1-2$ orders of magnitude larger value of the neutron EDM than the NDA formula does, in the $m(\tilde{d}_1) \sim 1$ TeV region. Therefore, a larger portion of the parameter space with new CP violating phases is excluded if we adopt the ChPT formula for the evaluation of the neutron EDM, and possible deviations in the CP violation observables are also affected.

In Fig. 16, we show the correlations between the neutron EDM calculated by the ChPT formula and the CP asymmetries $S_{CP}(B_d \to K^* \gamma)$, $\Delta S_{CP}(B_d \to \phi K_S)$, and $S_{CP}(B_s \to J/\psi\phi)$. The correlations between the neutron EDM and the LFV decay branching ratios are also shown. We show the correlation plots for the U(2) model in Fig. 17. In particular for the NDν_R(I)-NH and Dν_R-IH of the SU(5) SUSY GUT with right-handed neutrinos, the parameter region with large deviations of $\Delta S_{CP}(B_d \to \phi K_S)$ and

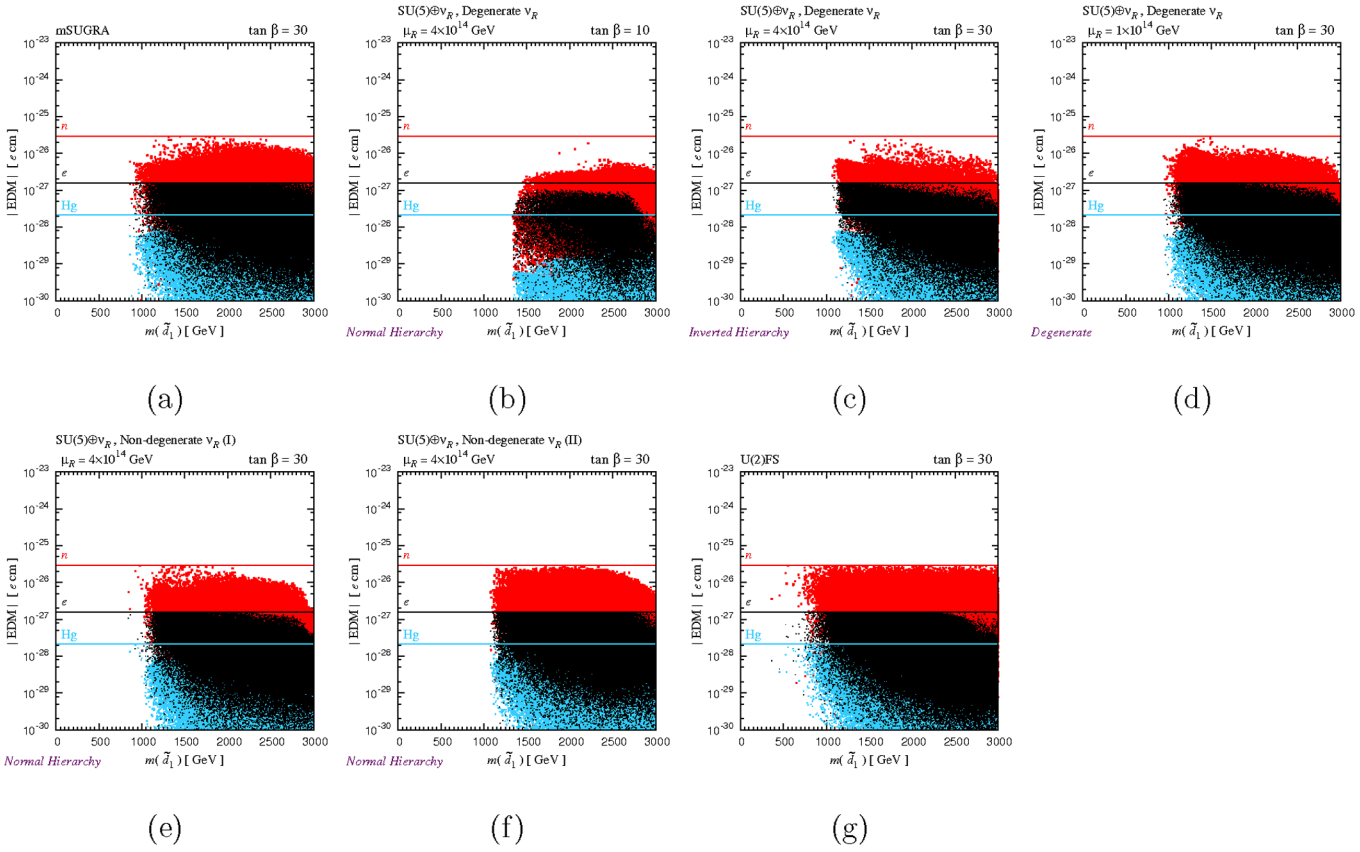

FIG. 14 (color online). Electric dipole moments of the neutron (gray/red), ^{199}Hg (light-gray/light-blue), and the electron (black) as functions of $m(\tilde{d}_1)$ for the same parameter sets as those in Fig. 6. Horizontal lines show the experimental upper limits. The neutron EDM is calculated by the NDA formula.

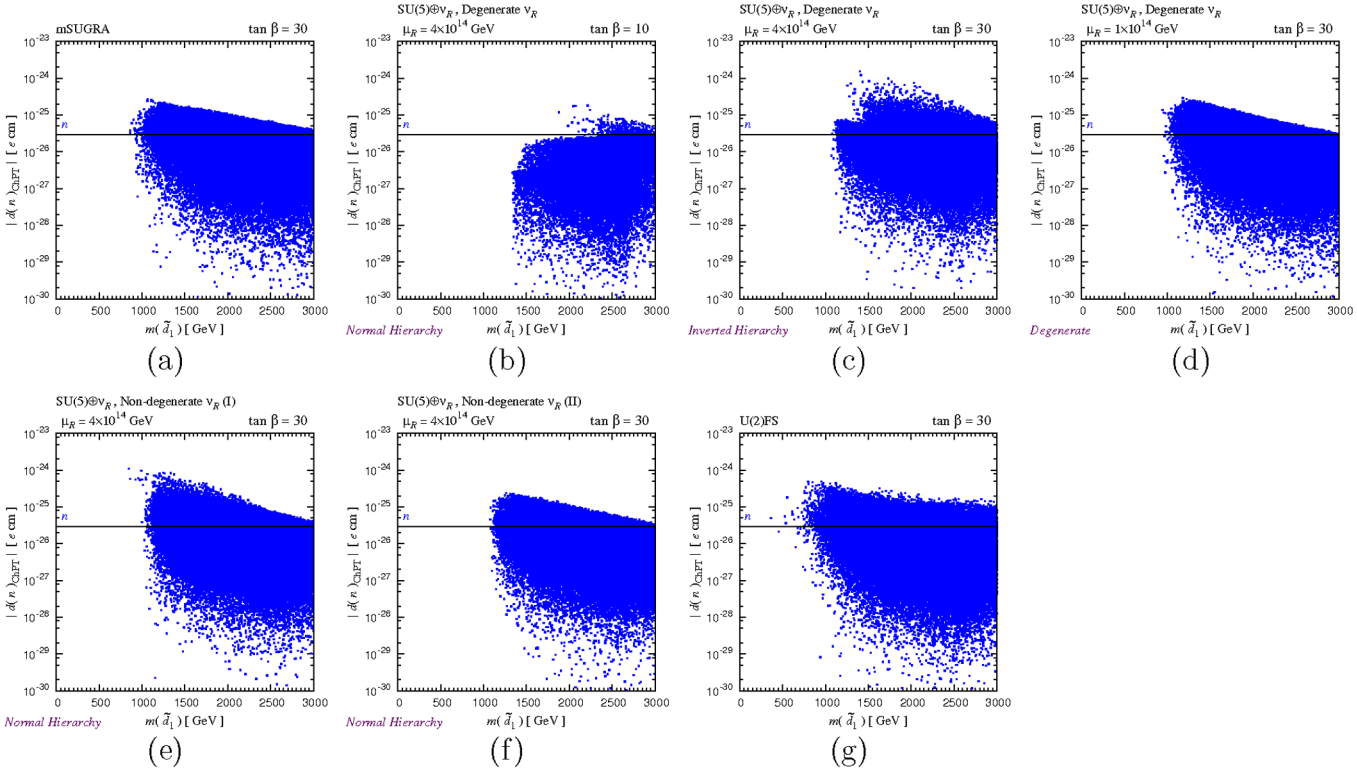

FIG. 15 (color online). The neutron EDM calculated by the ChPT formula for the same parameter sets as those in Fig. 14.

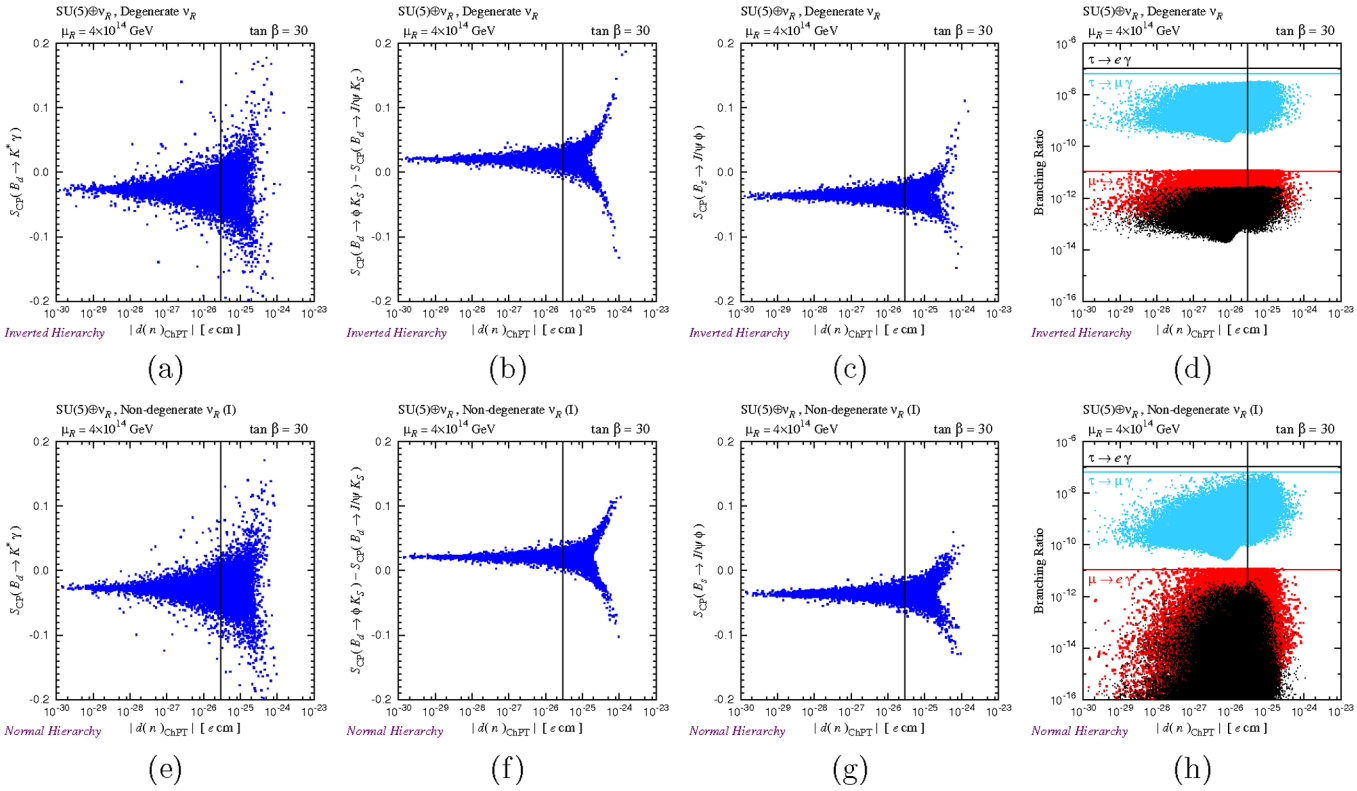

FIG. 16 (color online). The *CP* asymmetries in $b \to s$ decays and the LFV branching ratios as functions of the neutron EDM given by the chiral perturbation formula in SU(5) SUSY GUT with right-handed neutrinos. (a)–(d) and (e)–(h) are plots in the Dν_R-IH and the NDν_R(I)-NH cases, respectively.

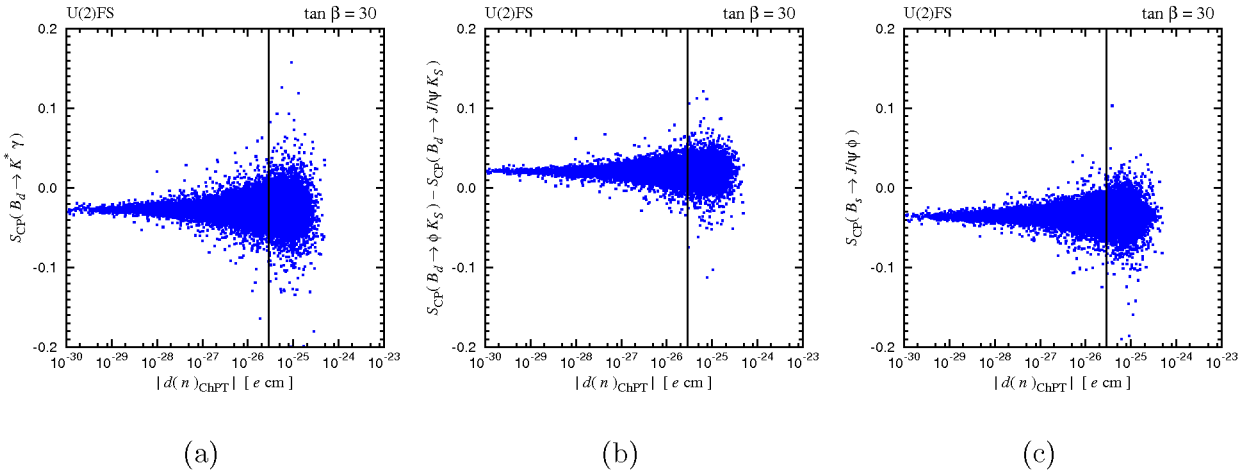

FIG. 17 (color online). The CP asymmetries in $b \to s$ decays as functions of the neutron EDM given by the chiral perturbation formula in the U(2) flavor symmetry model.

$S_{CP}(B_s \to J/\psi\phi)$ is excluded if we adopt the ChPT formula for the evaluation of the neutron EDM. On the other hand, large deviations remain for other cases.

D. Summary of results and experimental prospects

There are good experimental prospects for future improvements in the observables considered above. From recent study of Super B factories [66], the precision of determination for $50 - 75$ ab^{-1} is 0.02–0.03 for $S_{CP}(B_d \to K^*\gamma)$, 0.08–0.12 for $S_{CP}(B_d \to \rho\gamma)$, and 0.02–0.03 for $S_{CP}(B_d \to \phi K_S)$ for mixing-induced CP asymmetries. For the direct CP asymmetries of the radiative B decays, the expected sensitivity reaches 0.004 for $A_{\rm CP}(b \to s\gamma)$ and 0.01 for $A_{CP}(b \to (s+d)\gamma)$. The CP asymmetry of the $B_s \to J/\psi\phi$ mode is determined up to 0.01 from LHCb with 10 fb^{-1} [12]. The precision of the ϕ_3 determination is expected at 2.4° for LHCb at 10 fb^{-1} [12], and further improvement is expected at Super B factory. In order to extract a new physics effect from the correlation between $\Delta m_{B_s}/\Delta m_{B_d}$ and ϕ_3 we need to improve the determination of the ξ factor up to a percent level. The $\mu \to e\gamma$ branching ratio will be searched for at the 10^{-13} level at the MEG experiment. Current upper bounds of $\mathrm{B}(\tau \to \mu\gamma)$ and $\mathrm{B}(\tau \to e\gamma)$ are 6.8×10^{-8} and 1.1×10^{-7}, respectively, at the B factory experiments, and future improvement by $1 - 2$ orders of magnitude is expected at Super B factory.

Comparing with these prospects, we can determine the significance of the deviations observed in Figs. 3–12. Our results of lepton and quark flavor signals are summarized in Table V. We list various quark flavor signals in $b - s$ and $b - d$ transition for the mSUGRA, three cases of MSSM with right-handed neutrinos, and SU(5) SUSY GUT with right-handed neutrinos, and the U(2) flavor symmetry model. The μ and τ LFV processes are also included for the cases except for the U(2) model. The observable with a mark $\surd$ indicates that a large deviation is possible. The mark • means that there are some points that the deviation could be identified with future improvements of experimental measurements and/or theoretical understanding of uncertainty. From the table, we can see that significant flavor signals are expected in the lepton sector for the MSSM with right-handed neutrinos and the SU(5) SUSY GUT with right-handed neutrinos. These lepton flavor violation signals depend on the texture of the neutrino Yukawa coupling matrix, i.e., $\tau \to \mu\gamma$ can be large in Dν_R-IH, Dν_R-D, and NDν_R(I)-NH cases and $\tau \to e\gamma$ can be large in the NDν_R(II)-NH cases while satisfying the present experimental bound on $\mu \to e\gamma$. In Dν_R-NH cases, $\mu \to e\gamma$ is the most promising mode among these three lepton flavor violation processes. In the SU(5) SUSY GUT with right-handed neutrinos, in addition to the above texture dependent signals, $\mu \to e\gamma$ can be enhanced as large as the present experimental bound due to GUT interactions even in the nondegenerate ν_R (I) and (II) cases. As for the quark flavor signals, we can expect significant CP violating asymmetries in $b \to s$ and $b \to d$ transitions in the SU(5) SUSY GUT with right-handed neutrinos and in the U(2) model. The pattern of the deviations from the SM predictions also depends on the texture of the neutrino Yukawa coupling matrix in the SU(5) SUSY GUT with right-handed neutrinos. Examining the pattern of deviations from the SM in the quark and lepton flavor signals, we can gain insights on the flavor structure in the SUSY models.

In addition to experimental progress, it is important to reduce theoretical uncertainties to identify the deviations. In particular, the theoretical issue to predict mixing-induced CP asymmetries in $B_d \to K^*\gamma$ [67] and $B_d \to \phi K_S$ [68] modes within the SM needs to be clarified because the deviation we expect is up to 10% level.

Notice that the significant flavor signals in the models with right-handed neutrinos appear in the case with sufficiently large neutrino Yukawa couplings, which corre-

TABLE V. Summary of expected flavor signals for each model. "NH," "IH," and "D" denote normal hierarchy, inverted hierarchy, and degenerate, respectively, for the low-energy neutrino spectrum. The observable with a mark $\surd$ indicates that a large deviation is possible. The mark • means that there are some points that the deviation could be identified with future improvements of experimental measurements and/or theoretical understanding of uncertainty. We do not consider LFV processes for the U(2)FS model (−).

Model	$A_{CP}(s\gamma)$	$S_{CP}(K^*\gamma)$	$A_{CP}(d\gamma)$	$S_{CP}(\rho\gamma)$	$\Delta S_{CP}(\phi K_S)$	$S_{CP}(B_s \to J/\psi\phi)$	$\Delta m_{B_s}/\Delta m_{B_d}$ vs. ϕ_3	$\mu \to e\gamma$	$\tau \to \mu\gamma$	$\tau \to e\gamma$
mSUGRA										
MSSM + RN										
Degenerate ν_R, NH								$\surd$		
Degenerate ν_R, IH								$\surd$	$\surd$	
Degenerate ν_R, D								$\surd$	$\surd$	
Nondegenerate ν_R (I), NH									$\surd$	
Nondegenerate ν_R (II), NH										$\surd$
SU(5) + RN										
Degenerate ν_R, NH		•		•	•	•		$\surd$		
Degenerate ν_R, IH		$\surd$		•	$\surd$	$\surd$	•	$\surd$	$\surd$	
Degenerate ν_R, D		•		•	•	•		$\surd$	$\surd$	
Nondegenerate ν_R (I), NH		$\surd$			$\surd$	$\surd$	•	$\surd$	$\surd$	
Nondegenerate ν_R (II), NH				$\surd$			•	$\surd$		$\surd$
U(2)FS	$\surd$	$\surd$		$\surd$	$\surd$	$\surd$	•	—	—	—

sponds to the right-handed neutrino mass scale $\mu_R = O(10^{14})$ GeV. When we take a smaller value of μ_R, all the flavor signals are suppressed. As already mentioned, the effects of the neutrino Yukawa couplings are negligibly small for $\mu_R \ll 10^{12}$ GeV.

In this paper we do not include the heavy Higgs exchange contributions to various FCNC and LFV processes. These contributions are known to play an important role for particular cases of SUSY parameter sets due to large corrections to Yukawa coupling constants through SUSY loop diagrams [69]. The relevant parameter set corresponds to large values of $\tan\beta$ and relatively small values of heavy Higgs boson masses with large values of μ. The Higgs exchange contribution induces drastic effects in processes like $B_s \to \mu^+\mu^-$ and $b \to s l^+ l^-$ [70] especially for a large value of $\tan\beta$ ($= 50 - 60$) because of a high power dependence of $\tan\beta$. In some restricted parts of our analysis, we may have additional flavor signals due to the Higgs exchange effects.

IV. CONCLUSIONS

We have analyzed quark flavor signals associated with $b \to s$ and $b \to d$ transitions and lepton flavor violations in various cases of supersymmetric models. Extensive study is carried out in terms of observables for representative SUSY models. Our result is summarized in Table V. We have improved computational methods and updated phenomenological constraints from our works in previous publications. The most important effect is the inclusion of the constraint from the $B_s - \bar{B}_s$ mixing from recent Tevatron experiments. The maximum deviation for various $b \to s$ transition processes turns out to be the 10% level, compared to the previous results where the deviation at the level of 50% was possible. In this work, we also present predictions of tau lepton flavor processes. Under the constraint of $\mu \to e\gamma$, the tau LFV processes are promising to look for new physics effects, which are also related to $b \to s$ and $b \to d$ transition processes in SUSY GUT models. The pattern of deviation from the SM prediction provides us with an important clue on physics determining the structure of the SUSY breaking sector, and a future B factory plays a central role in such investigation along with ongoing flavor experiments such as MEG and LHCb.

ACKNOWLEDGMENTS

The work of T. G. and Y. O. is supported in part by the Grant-in-Aid for Science Research, Ministry of Education, Culture, Sports, Science and Technology, Japan, No. 16081211. The work of Y. O. is supported in part by the Grant-in-Aid for Science Research, Ministry of Education, Culture, Sports, Science and Technology, No. 17540286. The work of T. S. is supported in part by the INFN under the program "Fisica Astroparticellare," and by the Italian MIUR (Internazionalizzazione Program). The numerical calculations were carried out in part on Altix3700 BX2 at YITP in Kyoto University.

[1] N. Cabibbo, Phys. Rev. Lett. **10**, 531 (1963); M. Kobayashi and T. Maskawa, Prog. Theor. Phys. **49**, 652 (1973).

[2] Y. Ashie *et al.* (Super-Kamiokande Collaboration), Phys. Rev. D **71**, 112005 (2005); J. Hosaka *et al.* (Super-Kamkiokande Collaboration), Phys. Rev. D **73**, 112001 (2006); B. Aharmim *et al.* (SNO Collaboration), Phys. Rev. C **75**, 045502 (2007); M. Altmann *et al.* (GNO Collaboration), Phys. Lett. B **616**, 174 (2005); W. Hampel *et al.* (GALLEX Collaboration), Phys. Lett. B **447**, 127 (1999); J. N. Abdurashitov *et al.* (SAGE Collaboration), J. Exp. Theor. Phys. **95**, 181 (2002) [Zh. Eksp. Teor. Fiz. **122**, 211 (2002)].

[3] S. Yamamoto *et al.* (K2K Collaboration), Phys. Rev. Lett. **96**, 181801 (2006); M. H. Ahn *et al.* (K2K Collaboration), Phys. Rev. D **74**, 072003 (2006).

[4] T. Araki *et al.* (KamLAND Collaboration), Phys. Rev. Lett. **94**, 081801 (2005).

[5] M. Apollonio *et al.* (CHOOZ Collaboration), Eur. Phys. J. C **27**, 331 (2003); A. Piepke (Palo Verde Collaboration), Prog. Part. Nucl. Phys. **48**, 113 (2002).

[6] ATLAS Collaboration, Technical Design Report, Report No. CERN/LHCC/99-15, 1999; G. L. Bayatian *et al.* (CMS Collaboration), J. Phys. G **34**, 995 (2007).

[7] For reviews, see H. P. Nilles, Phys. Rep. **110**, 1 (1984); H. E. Haber and G. L. Kane, Phys. Rep. **117**, 75 (1985); S. P. Martin, arXiv:hep-ph/9709356; D. J. H. Chung, L. L. Everett, G. L. Kane, S. F. King, J. D. Lykken, and L. T. Wang, Phys. Rep. **407**, 1 (2005).

[8] J. R. Ellis and D. V. Nanopoulos, Phys. Lett. B **110**, 44 (1982).

[9] J. R. Ellis, S. Ferrara, and D. V. Nanopoulos, Phys. Lett. B **114**, 231 (1982).

[10] L. M. Barkov *et al.*, PSI Proposal Report No. R-99-05, 1999; S. Ritt (MEG Collaboration), Nucl. Phys. B, Proc. Suppl. **162**, 279 (2006).

[11] S. Amato *et al.* (LHCb Collaboration), Report Nos. CERN-LHCC-98-04, CERN-LHCC-P-4, 1998.

[12] T. Nakada, in Conference on Supersymmetry in 2010's, 2007, Hokkaido University, Sapporo, Japan (unpublished).

[13] A. G. Akeroyd *et al.* (SuperKEKB Physics Working Group), arXiv:hep-ex/0406071; S. Hashimoto *et al.*, Report No. KEK-REPORT-2004-4, 2004.

[14] M. Bona *et al.*, arXiv:0709.0451.

[15] J. L. Hewett *et al.*, arXiv:hep-ph/0503261.

[16] F. Gabbiani and A. Masiero, Nucl. Phys. **B322**, 235 (1989); I. I. Y. Bigi and F. Gabbiani, Nucl. Phys. **B352**, 309 (1991); J. S. Hagelin, S. Kelley, and T. Tanaka, Nucl. Phys. **B415**, 293 (1994).

[17] F. Gabbiani, E. Gabrielli, A. Masiero, and L. Silvestrini, Nucl. Phys. **B477**, 321 (1996); M. Ciuchini *et al.*, J. High Energy Phys. 10 (1998) 008; T. Besmer, C. Greub, and T. Hurth, Nucl. Phys. **B609**, 359 (2001); E. Lunghi and D. Wyler, Phys. Lett. B **521**, 320 (2001); D. Becirevic *et al.*, Nucl. Phys. **B634**, 105 (2002); S. Khalil and E. Kou, Phys. Rev. D **67**, 055009 (2003); Phys. Rev. Lett. **91**, 241602 (2003); G. L. Kane, P. Ko, H. B. Wang, C. Kolda, J. H. Park, and L. T. Wang, Phys. Rev. D **70**, 035015 (2004); Phys. Rev. Lett. **90**, 141803 (2003); M. Ciuchini, E. Franco, A. Masiero, and L. Silvestrini, Phys. Rev. D **67**, 075016 (2003); **68**, 079901(E) (2003); K. Agashe and C. D. Carone, Phys. Rev. D **68**, 035017 (2003); R. Harnik, D. T. Larson, H. Murayama, and A. Pierce, Phys. Rev. D **69**, 094024 (2004); J. Foster, K. I. Okumura, and L. Roszkowski, J. High Energy Phys. 08 (2005) 094.

[18] J. Foster, K. I. Okumura, and L. Roszkowski, Phys. Lett. B **641**, 452 (2006); M. Ciuchini and L. Silvestrini, Phys. Rev. Lett. **97**, 021803 (2006); M. Endo and S. Mishima, Phys. Lett. B **640**, 205 (2006).

[19] A. Bouquet, J. Kaplan, and C. A. Savoy, Phys. Lett. B **148**, 69 (1984); Nucl. Phys. **B262**, 299 (1985).

[20] L. J. Hall, V. A. Kostelecky, and S. Raby, Nucl. Phys. **B267**, 415 (1986).

[21] R. Barbieri and L. J. Hall, Phys. Lett. B **338**, 212 (1994).

[22] S. Bertolini, F. Borzumati, A. Masiero, and G. Ridolfi, Nucl. Phys. **B353**, 591 (1991); T. Goto, T. Nihei, and Y. Okada, Phys. Rev. D **53**, 5233 (1996); **54**, 5904(E) (1996); T. Goto, Y. Okada, and Y. Shimizu, arXiv:hep-ph/9908499; A. Bartl, T. Gajdosik, E. Lunghi, A. Masiero, W. Porod, H. Stremnitzer, and O. Vives, Phys. Rev. D **64**, 076009 (2001).

[23] S. Baek, T. Goto, Y. Okada, and K.-I. Okumura, Phys. Rev. D **63**, 051701 (2001); **64**, 095001 (2001).

[24] T. Moroi, J. High Energy Phys. 03 (2000) 019; Phys. Lett. B **493**, 366 (2000).

[25] R. Barbieri, L. J. Hall, and A. Strumia, Nucl. Phys. **B445**, 219 (1995); **B449**, 437 (1995); A. Masiero, M. Piai, A. Romanino, and L. Silvestrini, Phys. Rev. D **64**, 075005 (2001); N. Akama, Y. Kiyo, S. Komine, and T. Moroi, Phys. Rev. D **64**, 095012 (2001); J. Hisano and Y. Shimizu, Phys. Lett. B **565**, 183 (2003); **581**, 224 (2004); D. Chang, A. Masiero, and H. Murayama, Phys. Rev. D **67**, 075013 (2003); M. Ciuchini, A. Masiero, L. Silvestrini, S. K. Vempati, and O. Vives, Phys. Rev. Lett. **92**, 071801 (2004); M. Ciuchini, A. Masiero, P. Paradisi, L. Silvestrini, S. K. Vempati, and O. Vives, Nucl. Phys. **B783**, 112 (2007).

[26] L. Calibbi, A. Faccia, A. Masiero, and S. K. Vempati, Phys. Rev. D **74**, 116002 (2006).

[27] T. Goto, Y. Okada, Y. Shimizu, T. Shindou, and M. Tanaka, Phys. Rev. D **66**, 035009 (2002).

[28] T. Goto, Y. Okada, Y. Shimizu, T. Shindou, and M. Tanaka, Phys. Rev. D **70**, 035012 (2004).

[29] P. Ball and R. Fleischer, Eur. Phys. J. C **48**, 413 (2006); G. Isidori and P. Paradisi, Phys. Lett. B **639**, 499 (2006); S. Khalil, Phys. Rev. D **74**, 035005 (2006); S. Baek, J. High Energy Phys. 09 (2006) 077; R. Arnowitt, B. Dutta, B. Hu, and S. Oh, Phys. Lett. B **641**, 305 (2006); B. Dutta and Y. Mimura, Phys. Rev. Lett. **97**, 241802 (2006); S. Nandi and J. P. Saha, Phys. Rev. D **74**, 095007 (2006).

[30] J. Polchinski and M. B. Wise, Phys. Lett. B **125**, 393 (1983); Y. Kizukuri and N. Oshimo, Phys. Rev. D **45**, 1806 (1992); **46**, 3025 (1992); R. Barbieri, A. Romanino, and A. Strumia, Phys. Lett. B **369**, 283 (1996); T. Falk, K. A. Olive, and M. Srednicki, Phys. Lett. B **354**, 99 (1995); T. Falk and K. A. Olive, Phys. Lett. B **375**, 196 (1996); **439**, 71 (1998).

[31] T. Ibrahim and P. Nath, Phys. Lett. B **418**, 98 (1998); Phys. Rev. D **57**, 478 (1998); **58**, 019901(E) (1998); **60**, 079903(E) (1999); **60**, 119901(E) (1999); T. Goto, Y. Y. Keum, T. Nihei, Y. Okada, and Y. Shimizu, Phys. Lett. B

460, 333 (1999).
[32] D. Chang, W. Y. Keung, and A. Pilaftsis, Phys. Rev. Lett. **82**, 900 (1999); **83**, 3972 (1999).
[33] T. Falk, K. A. Olive, M. Pospelov, and R. Roiban, Nucl. Phys. **B560**, 3 (1999).
[34] P. Minkowski, Phys. Lett. B **67**, 421 (1977); M. Gell-Mann, P. Ramond, and R. Slansky, *Proceedings of the Supergravity Stony Brook Workshop, New York, 1979*, edited by P. Van Nieuwenhuizen and D. Freedman (North-Holland, Amsterdam, 1979); T. Yanagida, Proceedings of the Workshop on Unified Theories and Baryon Number in the Universe, Tsukuba, Japan, 1979, edited by A. Sawada and A. Sugamoto (KEK Report No. 79-18, 1979); R. N. Mohapatra and G. Senjanovic, Phys. Rev. Lett. **44**, 912 (1980).
[35] B. Pontecorvo, Sov. Phys. JETP **6**, 429 (1957) [Zh. Eksp. Teor. Fiz. **33**, 549 (1957)]; Sov. Phys. JETP **7**, 172 (1958) [Zh. Eksp. Teor. Fiz. **34**, 247 (1957)]; Sov. Phys. JETP **26**, 984 (1968) [Zh. Eksp. Teor. Fiz. **53**, 1717 (1967)]; Z. Maki, M. Nakagawa, and S. Sakata, Prog. Theor. Phys. **28**, 870 (1962).
[36] Y. Farzan, Phys. Rev. D **69**, 073009 (2004); Y. Farzan and M. E. Peskin, Phys. Rev. D **70**, 095001 (2004); Y. Farzan, J. High Energy Phys. 02 (2005) 025.
[37] F. Borzumati and A. Masiero, Phys. Rev. Lett. **57**, 961 (1986); J. Hisano, T. Moroi, K. Tobe, and M. Yamaguchi, Phys. Rev. D **53**, 2442 (1996); S. T. Petcov, S. Profumo, Y. Takanishi, and C. E. Yaguna, Nucl. Phys. **B676**, 453 (2004).
[38] J. R. Ellis, M. K. Gaillard, and D. V. Nanopoulos, Phys. Lett. B **88**, 320 (1979).
[39] A. Pomarol and D. Tommasini, Nucl. Phys. **B466**, 3 (1996); R. Barbieri, G. R. Dvali, and L. J. Hall, Phys. Lett. B **377**, 76 (1996); R. Barbieri and L. J. Hall, Nuovo Cimento A **110**, 1 (1997); R. Barbieri, L. Giusti, L. J. Hall, and A. Romanino, Nucl. Phys. **B550**, 32 (1999).
[40] R. Barbieri, L. J. Hall, and A. Romanino, Phys. Lett. B **401**, 47 (1997); R. Barbieri, L. J. Hall, S. Raby, and A. Romanino, Nucl. Phys. **B493**, 3 (1997).
[41] R. Barbieri, P. Creminelli, and A. Romanino, Nucl. Phys. **B559**, 17 (1999); T. Blažek, S. Raby, and K. Tobe, Phys. Rev. D **60**, 113001 (1999); **62**, 055001 (2000); A. Aranda, C. D. Carone, and R. F. Lebed, Phys. Lett. B **474**, 170 (2000); Phys. Rev. D **62**, 016009 (2000); M. C. Chen and K. T. Mahanthappa, Phys. Rev. D **62**, 113007 (2000); A. Aranda, C. D. Carone, and P. Meade, Phys. Rev. D **65**, 013011 (2001); S. Raby, Phys. Lett. B **561**, 119 (2003).
[42] S. P. Martin and M. T. Vaughn, Phys. Rev. D **50**, 2282 (1994); Y. Yamada, Phys. Rev. D **50**, 3537 (1994); I. Jack and D. R. T. Jones, Phys. Lett. B **333**, 372 (1994); I. Jack, D. R. T. Jones, S. P. Martin, M. T. Vaughn, and Y. Yamada, Phys. Rev. D **50**, R5481 (1994).
[43] D. M. Pierce, J. A. Bagger, K. T. Matchev, and R. J. Zhang, Nucl. Phys. **B491**, 3 (1997).
[44] M. Okamoto, Proc. Sci., LAT2005 (**2006**) 013 [arXiv:hep-lat/0510113]; C. R. Allton *et al.*, Phys. Lett. B **453**, 30 (1999); D. Becirevic, V. Gimenez, G. Martinelli, M. Papinutto, and J. Reyes, J. High Energy Phys. 04 (2002) 025.
[45] B. Kayser, M. Kuroda, R. D. Peccei, and A. I. Sanda, Phys. Lett. B **237**, 508 (1990); I. Dunietz, H. R. Quinn, A. Snyder, W. Toki, and H. J. Lipkin, Phys. Rev. D **43**, 2193 (1991).
[46] N. G. Deshpande, X. G. He, and J. Trampetic, Phys. Lett. B **377**, 161 (1996); R. Barbieri and A. Strumia, Nucl. Phys. **B508**, 3 (1997); R. Fleischer, Z. Phys. C **58**, 483 (1993); **62**, 81 (1994).
[47] A. L. Kagan and M. Neubert, Phys. Rev. D **58**, 094012 (1998).
[48] C. Greub, T. Hurth, and D. Wyler, Phys. Lett. B **380**, 385 (1996); Phys. Rev. D **54**, 3350 (1996); N. Pott, Phys. Rev. D **54**, 938 (1996).
[49] D. Atwood, M. Gronau, and A. Soni, Phys. Rev. Lett. **79**, 185 (1997).
[50] S. Weinberg, Phys. Rev. Lett. **63**, 2333 (1989).
[51] J. Hisano and Y. Shimizu, Phys. Rev. D **70**, 093001 (2004); J. Hisano, M. Kakizaki, M. Nagai, and Y. Shimizu, Phys. Lett. B **604**, 216 (2004).
[52] S. Kanemura, K. Matsuda, T. Ota, T. Shindou, E. Takasugi, and K. Tsumura, Phys. Rev. D **72**, 055012 (2005); **72**, 059904(E) (2005); S. T. Petcov, T. Shindou, and Y. Takanishi, Nucl. Phys. **B738**, 219 (2006); S. T. Petcov and T. Shindou, Phys. Rev. D **74**, 073006 (2006).
[53] A. Heister *et al.* (ALEPH Collaboration), Phys. Lett. B **526**, 206 (2002); **583**, 247 (2004); J. Abdallah *et al.* (DELPHI Collaboration), Eur. Phys. J. C **31**, 421 (2004); P. Achard *et al.* (L3 Collaboration), Phys. Lett. B **580**, 37 (2004); G. Abbiendi *et al.* (OPAL Collaboration), Eur. Phys. J. C **32**, 453 (2004); S. Schael *et al.* (LEP Collaborations, ALEPH, DELPHI, L3, OPAL, and LEP Working Group for Higgs Boson Searches), Eur. Phys. J. C **47**, 547 (2006); A. A. Affolder *et al.* (CDF Collaboration), Phys. Rev. Lett. **88**, 041801 (2002); M. Martinez-Perez (CDF Collaboration), AIP Conf. Proc. **903**, 189 (2007); V. M. Abazov *et al.* (D0 Collaboration), Phys. Lett. B **638**, 119 (2006).
[54] P. Koppenburg *et al.* (Belle Collaboration), Phys. Rev. Lett. **93**, 061803 (2004); B. Aubert *et al.* (*BABAR* Collaboration), Phys. Rev. D **72**, 052004 (2005); S. Chen *et al.* (CLEO Collaboration), Phys. Rev. Lett. **87**, 251807 (2001).
[55] M. Ahmed *et al.* (MEGA Collaboration), Phys. Rev. D **65**, 112002 (2002).
[56] B. Aubert *et al.* (*BABAR* Collaboration), Phys. Rev. Lett. **95**, 041802 (2005).
[57] B. Aubert *et al.* (*BABAR* Collaboration), Phys. Rev. Lett. **96**, 041801 (2006).
[58] M. V. Romalis, W. C. Griffith, and E. N. Fortson, Phys. Rev. Lett. **86**, 2505 (2001).
[59] C. A. Baker *et al.*, Phys. Rev. Lett. **97**, 131801 (2006).
[60] B. C. Regan, E. D. Commins, C. J. Schmidt, and D. DeMille, Phys. Rev. Lett. **88**, 071805 (2002).
[61] E. Barberio *et al.* (Heavy Flavor Averaging Group (HFAG) Collaboration), arXiv:0704.3575.
[62] A. Abulencia *et al.* (CDF Collaboration), Phys. Rev. Lett. **97**, 242003 (2006).
[63] J. L. Feng, K. T. Matchev, and T. Moroi, Phys. Rev. D **61**, 075005 (2000).
[64] M. Drees and M. M. Nojiri, Phys. Rev. D **47**, 376 (1993); S. Mizuta and M. Yamaguchi, Phys. Lett. B **298**, 120 (1993); J. Edsjö and P. Gondolo, Phys. Rev. D **56**, 1879 (1997); J. L. Feng, K. T. Matchev, and F. Wilczek, Phys.

Lett. B **482**, 388 (2000).

[65] J. R. Ellis, T. Falk, and K. A. Olive, Phys. Lett. B **444**, 367 (1998).

[66] T. E. Browder, M. Ciuchini, T. Gershon, M. Hazumi, T. Hurth, Y. Okada, and A. Stocchi, arXiv:0710.3799.

[67] B. Grinstein, Y. Grossman, Z. Ligeti, and D. Pirjol, Phys. Rev. D **71**, 011504 (2005); M. Matsumori and A. I. Sanda, Phys. Rev. D **73**, 114022 (2006); P. Ball and R. Zwicky, Phys. Lett. B **642**, 478 (2006).

[68] Y. Grossman, G. Isidori, and M. P. Worah, Phys. Rev. D **58**, 057504 (1998); M. Beneke, Phys. Lett. B **620**, 143 (2005); A. R. Williamson and J. Zupan, Phys. Rev. D **74**, 014003 (2006); **74**, 03901(E) (2006).

[69] L. J. Hall, R. Rattazzi, and U. Sarid, Phys. Rev. D **50**, 7048 (1994); K. S. Babu and C. F. Kolda, Phys. Lett. B **451**, 77 (1999); M. S. Carena, D. Garcia, U. Nierste, and C. E. M. Wagner, Nucl. Phys. **B577**, 88 (2000).

[70] C. S. Huang, W. Liao, and Q. S. Yan, Phys. Rev. D **59**, 011701 (1998); C. Hamzaoui, M. Pospelov, and M. Toharia, Phys. Rev. D **59**, 095005 (1999); S. R. Choudhury and N. Gaur, Phys. Lett. B **451**, 86 (1999); K. S. Babu and C. F. Kolda, Phys. Rev. Lett. **84**, 228 (2000).